Smart delivery systems for microbial biofilm therapy: Dissecting design, drug release and toxicological features

A. Sousa , A. Ngoc Phung , N. Škalko-Basnet , S. Obuobi [*]

Drug Transport and Delivery Research Group, Department of Pharmacy, UIT The Arctic University of Norway, Tromsø, Norway

A R T I C L E   I N F O

A B S T R A C T

Bacterial biofilms are highly protected surface attached communities of bacteria that typically cause chronic infections. To address their recalcitrance to antibiotics and minimise side effects of current therapies, smart drug carriers are being explored as promising platforms for antimicrobials. Herein, we briefly summarize recent efforts and considerations that have been applied in the design of these smart carriers. We guide readers on a journey on how they can leverage the inherent biofilm microenvironment, external stimuli, or combine both types of stimuli in a predictable manner. The specific carrier features that are responsible for their 'on-demand' properties are detailed and their impact on antibiofilm property are further discussed. Moreover, an analysis on the impact of such features on drug release profiles is provided. Since nanotechnology represents a significant slice of the drug delivery pie, some insights on the potential toxicity are also depicted. We hope that this review inspires researchers to use their knowledge and creativity to design responsive systems that can eradicate biofilm infections.

1. Introduction

Since Alexander Fleming discovered penicillin in 1928 and the mass production of the antibiotic began in the 1940's, millions of lives have been saved from the deadly effects of infectious diseases [1,2]. In recent years however, pathogenic microbes have adapted to develop resistance against many of our antimicrobial arsenal; a phenomenon commonly known as antimicrobial resistance (AMR). These microbes can also survive the host defenses as well as other external stresses by developing biofilms [3,4]. Biofilms are described as small structural dynamic communities of microbial cells (*e.g.*, fungal, and bacterial species), that excrete an extracellular polymeric substance also called the exopolysaccharide (EPS). The EPS, composed of proteins, lipids, enzymes and extracellular DNA forms a crucial self-generated and very much protective heterogenous environment called the extracellular matrix, biofilm matrix or EPS matrix (Fig. 1A) [5,6].

The matrix contributes to the high virulence and tolerance of biofilms to antibiotics by restricting drug penetration, diffusion and limiting the retention of antibiotics [7]. Within the matrix, a unique microenvironment forms where slow growing cells thrive. Consequently, biofilms are 10–1000 more tolerant to antibiotics compared to their free motile planktonic cells [8]. While the components of the

matrix may vary among microbes, their adherent features and ability to colonize different surfaces and tissues remains common [9]. This includes medical devices such as sutures, catheters, and dental implants, as well as tissues (*e.g.*, skin wounds). Additionally, some bacteria possess the ability to form biofilms in the air-liquid interface (also termed pellicle or floating biofilm) [10]. Biofilm formation is involved in the pathogenesis of many diseases and is responsible for up to 80% of all human bacterial infections [11]. Pathogens frequently associated with biofilms include *Pseudomonas aeruginosa*, *Staphylococcus aureus, Escherichia coli,* and *Candida albicans* [12]. Because biofilm infections are highly recalcitrant to antimicrobials, they persist and are major causes of treatment failure in clinics. With increasing global interest in AMR, a significant number of clinical isolates bearing drug-resistant genes to last line antibiotics have been identified [13] and the risk to form biofilm communities further amplifies the AMR burden. Biofilm formation is broadly regarded as a 5 stages process that can be briefly summarized by bacterial adherence, biofilm growth and final dispersion. The first stage consists of the migration and adherence of free motile cells to a designated surface where they start to produce EPS (stage two), aggregate densely, and form the matrix. Biofilm maturation starts in stage three, where microcolonies and water channels are formed. Full maturity is achieved in stage four, where the bacterial community is at its maximum

---

* Corresponding author.
  E-mail address: sybil.obuobi@uit.no (S. Obuobi).

cell density. In the final stage, the microcolonies are released from the biofilm and migrate to different surfaces [12]. However, this conceptual model does not fully address aggregated bacteria that do not attach to a hard surface which are also often involved in clinical and environmental settings. Suspended biofilm-like aggregates have been shown to embed in host materials such as mucus and sloughs from wounds. For free-floating aggregates, five mechanisms have also been highlighted that describe their formation. This includes the detachment of surface attached biofilms, growth of aggregates in the planktonic phase, growth of aggregates initiated through cell surface components of single cells, aggregation with host polymers *via* a mechanism known as depletion aggregation or binding of bacteria to molecules in host fluids through surface adhesion interactions. The reader is referred to a recent excellent review that discusses in detail these mechanisms [14].

2. Biofilm environment

Microbes survive antibiotic therapy by altering their drug targets, overexpressing efflux pumps, producing degrading enzymes or mutating target genes [15]. These mechanisms are widely associated with planktonic microbes but can also be observed in the biofilm state (Fig. 1B). In biofilms, communities of bacteria adhere to biotic or abiotic surfaces and embed themselves in a hydrated matrix (termed the extra-polymeric substance (EPS)) [16]. Similar observations have been made

in several species of yeast and filamentous fungi. A switch from the yeast state to the hyphae state in *Candida albicans* and *Exophiala dermatitidis* is recognised as a virulence factor and linked to biofilm formation [17]. EPS production during biofilm formation contributes to the intrinsic resistance of biofilm communities. Additionally, the presence of dormant cells, their spatial heterogeneity within the biofilm, quorum sensing, and other stress responses are vital to biofilm recalcitrance (Fig. 1B) [18,19].

2.1. EPS matrix

The EPS matrix is complex and makes up around 90% of the biofilm biomass [20]. It is described as a 'protective clothing' that shelters bacterial cells from environmental stress, structurally supports it and functions to mediate intercellular communication [21]. The matrix is mainly made up of polysaccharides, lipids, proteins, and extracellular DNA (eDNA) which hinder the transport of antimicrobial agents. As a result, sublethal doses reach the deeper layers of the biofilm and contribute to the decreased activity of antimicrobial drugs. In a recent study, Davenport and co-workers demonstrated that EPS from *A. baumannii* inhibited the activity of tobramycin *via* physical interactions but highlighted that the addition of cations reduced this protective effect [22]. This feature was also reported by Billings *et al* who showed that the ability of Psl (a major polysaccharide in the biofilm
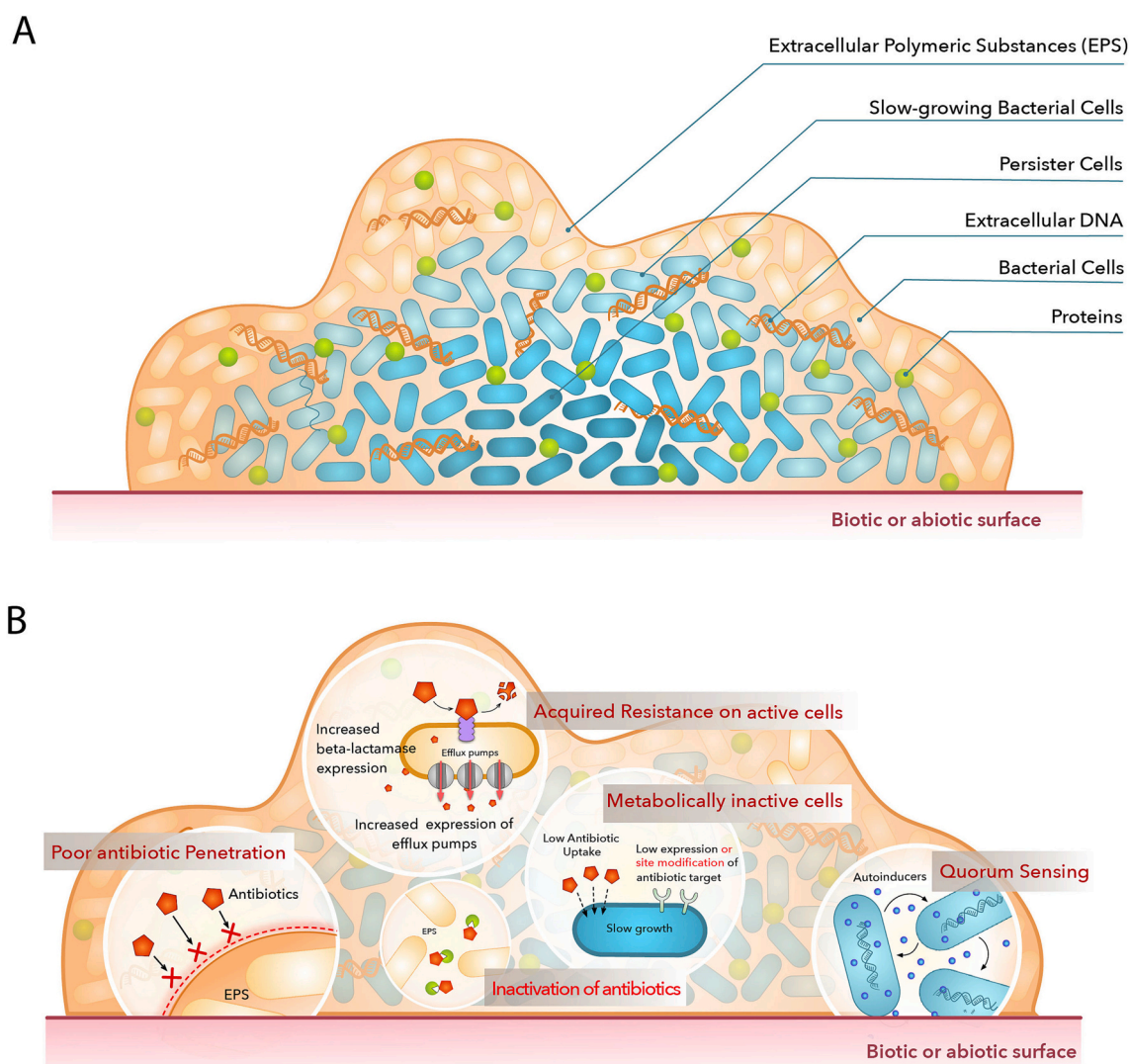

Fig. 1. Schematic diagram of biofilms and their resistance mechanisms. A) Major composition of biofilms. B) Major resistance mechanisms in biofilms.

matrix of *P. aeruginosa*) to sequester antibiotics can be supressed in the presence of high sodium chloride concentrations [23]. It was proposed that the neutrally charged Psl forms complexes with other anionic components of the matrix, highlighting existing interactions between components of the matrix as contributors to the intrinsic tolerance of biofilms. In fungal biofilms, the EPS was also found to prevent the penetration of antifungals *via* drug binding [24].

Additionally, microcolonies embedded within the EPS are interspersed by void areas or water channels that transport nutrients and waste metabolites. Although the exact size of the pores is difficult to estimate, an effective size range of 50 nm for loose flocs or below 10 nm for dense biofilms was reported in *P. fluorescens* [25]. Additionally, thick and highly confluent biofilms with dense microcolonies and small water-channel-like voids were formed at high sucrose concentrations in *S. mutans* [26]. In view of this, artificial channels were created in infectious biofilms using magnetic-iron-oxide nanoparticles to enhance the efficacy of antibiotics [27]. Through the creation of artificial channels perpendicular to the substratum surface, improved antimicrobial efficacy of gentamycin (4- to 6-fold) was observed. Other means to disassemble the EPS matrix involve the use of natural enzymes such as DNases, proteases and alginases [28]. Treatment of biofilms with deoxyribonucleases or proteases causes hydrolysis of the phosphodiester bonds of DNA or proteolysis of matrix proteins/adhesins in the EPS matrix respectively. Therapeutically, treatment with DNase I resulted in the marked reduction of biofilm adhesion and structural stability in *Vibrio parahaemolyticus* biofilms [29]. Similar observations were made in *S. aureus* and *P. aeruginosa* mixed species biofilms, where combined treatment with trypsin and, DNase I led to a significant reduction in the minimum biofilm eradication concentrations (MBEC) of meropenem and amikacin alongside potent biofilm dispersal and dissolution [30].

2.2. Quorum sensing

Quorum sensing (QS) is defined as a cell communication mechanism wherein the secretion of chemical signals (*e.g.*, autoinducing peptides (AIPs), homoserine lactones) activates genes that mediate cell motility, virulence, competence, and biofilm development [31,32]. Microbial cells within biofilm communities also adopt QS mechanisms to coordinate cell proliferation, sustenance and dissemination [33]. The imperative role of QS in biofilm development and virulence has drawn attention to the identification of new antibiofilm strategies of eukaryotic and prokaryotic origin [33,34]. Because QS directly controls bacteria cell population [35], disruption of this signalling pathway is a viable means to lower the selection pressure of bacteria. This has a direct implication in regulating the expression of virulence factors and in preventing the development of pathogenic biofilms [36]. Within this context, the use of quorum sensing inhibitors has been proposed as a strategy to enhance biofilm susceptibility to antibiotic therapy. For instance, cinnamic acid derivatives were shown to markedly inhibit biofilm formation and enhance tobramycin susceptibility [37]. Conversely and in fungal cells, Ramage and co-authors described the inhibition of hyphae development during the initial stage of *C. albicans* biofilm formation after treatment with the quorum sensing molecule Farnesol [38].

2.3. Persister cells

Pathogenic microorganisms form biofilms as they adapt to stressful conditions (*e.g.*, nutrient limitations). Within the biofilm matrix, a subpopulation of cells emerge that enter a resting stage of persistence. Unlike resistant cells that survive exposure to antibiotics, these metabolically inactive cells tolerate antibiotic exposure due to their physiological state of dormancy [39]. Without undergoing genetic mutations, these cells can survive for long periods because most antibiotics have cellular targets in dividing cells. As a result, populations of persister cells are major contributors of relapsing infections [40]. In a bid to kill

persister cells, various approaches have been explored, such as direct killing of the sleeping cells *via* the application of agents that do not require any cell machinery (*e.g.*, mitocin C and cisplastin) [41,42]. Along the same lines, antimicrobial peptides can exert action against different sub-populations irrespective of the metabolic stage. In this way, preformed biofilms harbouring high percentages of persister cells were successfully dispersed and killed following treatment with AMPs with arginine and tryptophan repeat units [43]. Alternatively, the addition of sugars and glycolysis intermediates can be applied to wake up sleeping cells for subsequent antibiotic treatment [44].

3. Smart materials as carriers for biofilm therapy

The modulation of the physicochemical properties of drug delivery systems (DDS) holds tremendous potential in improving the biological fate of therapeutic cargos against infectious diseases. Panels of studies have demonstrated the impact of nanoparticle size, shape, and surface properties in enhancing antibacterial properties [45–49]. Besides, the temporarily dilated and leaky blood vessels around infected cutaneous injuries (due to the enhanced permeability effect) has encouraged the passive accumulation of polymeric nanoparticles injected *in vivo* [50]. However, improved nanoparticle penetration/accumulation is only effective if high concentrations of the antimicrobial are available within the infection site. Equally so, the timely release of the antimicrobial is critical as the mere presence of the nanoparticle may especially have no impact on slow-growing cells within the biofilm. Additionally, in other pathological conditions such as infective endocarditis, targeted antimicrobial formulations are fundamental to eradicate pathogens and limit high-risk surgical intervention [51]. Therefore, maintaining the right concentration gradient of the free antimicrobial agent *via* the use of engineered smart drug delivery systems that are reliably activated in response to specific stimuli is crucial to achieve therapeutic success.

Concordantly, these materials aid nanoparticle navigation in the body and provide an avenue to overcome low on-target bioavailability, sub-therapeutic drug accumulation in microbial sanctuary and low patient compliance due to drug toxicity [52]. Smart materials (also referred to as intelligent or environmentally responsive materials) have attracted immense attention in this regard for use as carriers in drug delivery, imaging and in the development of sensors [53–55]. The stimulation of these materials in response to specific internal stimuli that differentiates the bacterial microenvironment from normal cells in humans (*e.g.*, pH, ionic strength, elevated enzymes/toxins and oxidative stress) can be exploited for controlled release of antimicrobial cargos [56]. At the same time, parallel efforts have been invested in applying external stimuli such as light, electrical, and magnetic field to improve the performance of passively/actively targeting antimicrobial nanomedicines or to generate other local stimuli that promote disruption of the biofilm.

In this review, we analyze drug delivery systems that respond to internal or external stimuli for a triggered drug release against biofilms. We discuss the features behind these mechanisms and how they improve biofilm penetration and destruction. Additionally, an analysis on how the responsiveness impacts drug release and effectiveness against biofilm destruction is provided. Finally, a brief section on toxicity of the systems is portrayed. There are excellent reviews that discuss current progress on stimuli-responsive systems but don't distinguish between their antibiofilm and antibacterial applications (*i.e.*, discuss applications against both biofilm and planktonic bacteria) [57–59]. Owing to the impact of the biofilm matrix and its unique microenvironment to drug tolerance and recurrence of infection, this review narrows the literature to biofilm therapy by accessing how these carriers eradicate and/or inhibit biofilms. The construction of stimuli-responsive nanocarrier for bacterial biofilm destruction has been reviewed elsewhere [60] yet, to the best of our knowledge, this is the first review to address stimuli-responsive delivery systems against both bacterial and fungal biofilms. Moreover, to guide translational efforts, this review additionally

provides an analysis on how drug release is influenced and discusses relevant toxicity concerns. We anticipate that the development of multi-responsive nanocarriers holds immense potential to favourably interact with biofilms and improve the efficacy of conventional antibiotics. This review aims to engage and inspire scientists in developing highly efficient nanocarriers towards the fight against recalcitrant biofilm infections.

4. Drug delivery systems responding to bacterial microenvironment

4.1. pH-responsive

Polymeric systems with pH-responsive properties alter their size, shape or surface chemistry in response to solution pH [61]. These carriers contain ionizable acidic or basic residues (*e.g.*, carboxyl, pyridine, sulfonic, phosphate and tertiary amine) that can donate or accept protons [61]. Common strategies that impart pH responsiveness include the fabrication of polymers with charge shifting properties or acid labile linkages. In the first instance, charge shifting systems prepared with hydrophobic polymers (*e.g.*, poly (B-amino ester), poly(4-vinyl pyridine)) revert to a cationic and hydrophilic state while hydrophilic polymers such as poly(propyl acrylic acid) become more hydrophobic when the pH of the solution drops [62,63]. On the other hand, polymeric systems with pH labile linkages such as hydrazone, imine, or acetal/ketal show enhanced hydrolysis at low pH environments [64–68]. A summary of pH-responsive systems, as well as the specific stimuli-responsive functions can be found in Table 1 and representative examples are illustrated in Fig. 2. On the premise of enhancing nanoparticle stability, the synthesis of crosslinkers with charge shifting or acid labile moieties (*e.g.*, ethylene glycol dimethacrylate, disulfide) can be explored [69,70]. Following ionic/non-ionic transition, these polymeric systems self-assemble, precipitate, swell or (de)swell to control drug release, cellular uptake, or binding affinity. Owing to the unique acidic pH within infection sites, these nanocarriers have potential applications for site-specific antimicrobial activity with minimal toxicity.

Surface modified nanoporous silica nanoparticles prepared with poly (4-vinylpyridine) were developed for the delivery of chlorhexidine by Fullriede et al. The carrier showed a cationic surface potential under acidic conditions (due to the protonation of the pyridine groups). An increasing amount of chlorhexidine was released over 5 days irrespective of pH value, however the authors observed higher amounts in acidic conditions. A comparison between unmodified particles and the responsive carrier showed that the coating reduced the amount of chlorhexidine released over time in neutral conditions. Still, antibacterial activity in acidogenic *S. mutans* was also observed at high pH conditions using the resazurin assay. This was attributed to uncontrolled leaching of chlorhexidine [74]. Considering the impact of short and inaccurate doses of antimicrobials on the development of resistance, tailoring drug release is essential for such systems. To enhance drug retention and promote affinity of these materials, Niaz and colleagues developed a mucoadhesive coacervate system using sodium caseinate and sodium alginate [75]. The nanocarrier demonstrated high entrapment ($75.1 \pm 1.2\%$) of nisin at acidic pH with significantly enhanced muco-absorption due to the cationic charge of casein at acidic pH. Although the authors demonstrated rapid release of nisin in simulated salivary fluid (pH 6.8), comparative release at physiological pH was not assessed. After 24 h exposure of the formulation, biofilm inhibition assays demonstrated up to 65% inhibition of *S. epidermidis* biomass production and a marked increase to almost 100% inhibition was observed at 48 h. Similar high inhibition of *E. faecium* (90%) and *E. faecalis* (84%) was seen with the nano-antimicrobials after 48 h. Free nisin on the other hand achieved only 45%, 25% and 32% inhibition in *S. epidermidis, E. faecium* and *E. faecalis*. The biomass inhibition of free nisin did not increase much after 48 h.

To improve these observations, biominerals such as calcium carbonate and calcium phosphate maintain a robust structure under physiological pH and dissociate to ionic species under acidic pH. Therefore Min and colleagues developed a nanoparticulate system for the topical release of antibiotics against oral biofilms [71]. Using a polyethyleneglycol-polyaspartate (PEG-PAsp) templated mineralization method, a CaCO$_3$ core was formed wherein the anionic Pasp promoted the nucleation and growth of the mineralized core with simultaneous loading of doxycycline. The authors reported that the mineral core inhibited the leakage of entrapped doxycycline (19.8% release at pH 7.4 over 24 h) under normal salivary pH conditions. Conversely, a significant release of doxycycline and calcium was recorded at acid pH conditions (pH 6.5, 5.5. and 4.5) triggered by the accelerated decomposition of the mineral core into ionic species with high potency against *Prevotella intermedia* biofilms. This observation was attributed to the exponential increase of the solubility of CaCO$_3$ in aqueous solution at low pH conditions. Moreover, both a decrease in biofilm formation at a controlled acidic pH and inhibitory effect against preformed biofilms were observed with the formulation, assessed with crystal violet staining assay and confocal images, respectively. At the highest (170 μg/mL) dose of the nanoparticles, >40% inhibition of biofilm formation was observed in controlled pH conditions.

Numerous pH-responsive carriers that rely on inherent charge-shifting properties, have also been investigated for biofilm therapy. A study by Hassan and colleagues recently studied a novel oleylamine based zwitterionic nanovesicle for the delivery of vancomycin against MRSA biofilms [76]. A switch in surface charge of the vesicles from -6.97 ± 6.5 mV (pH 7.4) to $+13.3 \pm 1.75$ mV (pH 6.0) was observed due to the protonation of the secondary amines in oleylamine. Correspondingly, *in vitro* drug release demonstrated $92.12 \pm 1.1.\%$ released vancomycin at pH 6.0 whereas, $73.22 \pm 0.02\%$ drug release was reported after 72 h at pH 7.4. Moreover 95-fold lower MRSA burden was observed *in vivo* compared to the free vancomycin using colony counting on agar plates with the homogenized skin tissues. Zhao and co-workers fabricated a pH-responsive nanocarrier for chlorhexidine delivery [77]. In this work, core-shell polyionic complex micelles were prepared using citraconic anhydride modified polymers. Drug loading of the cationic chlorhexidine was achieved *via* electrostatic interactions. Degradation of citraconic amine groups was shown to be sensitive to acidic pH with the disassembly of the micelles and release of chlorhexidine. Using confocal microscopy, *in vitro* release assessment revealed 69% chlorhexidine was released after 3 h under acidic environments alongside efficient killing of *Steptococcus mutans* biofilms. Another lipid-based delivery system was used by Zhou *et al* [78] wherein quaternary ammonium salt of chitosan was electrostatically adsorbed onto liposomes for the delivery of doxycycline. Protonation of the residual amines on the chitosan coating at acidic pH led to half-time release of 0.75 h and 2.3 h respectively at pH 4.5 and 6.8 respectively. Here assessment of the release profile at physiological pH was unfortunately not performed. Nevertheless, these effects were confirmed through the observation of a zeta potential shift -9.08 mV (physiological pH) to $+8.92$ mV (pH 4.5), as well as the observation of a burst release of drug content at acidic pH when compared to a pH of 6.8. It is however noted that the observed burst release was prominent only within the first 4 h of the studies after which there was not much difference between the release profiles. On the other hand, the carriers achieved biofilm disruption (evaluated with scanning electron microscopy, crystal violet staining and confocal microscopy) without significant signs of toxicity to the osteoblastic cell line, MC3T3-E1. Liu and colleagues recently described the preparation of a surface adaptable micellar system for the delivery of a hydrophobic compound triclosan [79]. To achieve this, the authors compared mixed-shell-polymeric-micelles (MSPM) with single-shell-polymeric-micelles (SSPM) wherein the former carrier possessed a shell comprising poly (ethylene glycol) and a poly(β-amino ester) (PAE), while the later lacked the PAE function (responsible for the pH-triggered action). The authors demonstrated the surface adaptable features of the mixed shell system due to protonation of the PAE group at a pH of 5.0, a phenomenon not

Table 1

Internally-responsive drug delivery systems.

| Trigger	Active compound	Stimuli responsive function	Core Material / System	Purpose	Reference
pH	Chlorhexidine	Poly(4-vinylpyridine)	Nanoporous silica	The polymer becomes protonated at acidic pH, creating pores between the chains due to electrostatic repulsion allowing for drug release	[74]
	Nisin (antimicrobial peptide)	Casein	Protein and polysaccharide nano-coacervate	Casein is positively charged at acidic pH, and at simulated salivary fluid (pH 6.8), the decrease in the positive charges reduces the stabilization between casein and sodium alginate, releasing the nisin	[75]
	Doxycycline	Calcium carbonate	Calcium carbonate nanoparticles	At acidic pH, the mineralized nanoparticles dissociate to ionic species and release the loaded drug	[71]
	Vancomycin	Oleylamine based zwitterionic lipid	Chitosan-lipid hybrid nanovesicles	Acidic environment results in protonation of nitrogen atoms in mine group of oleylamine and chitosan, causing repulsion between lipid and polymer and a system disturbance	[76]
	Chlorhexidine	poly(2-(((2-aminoethyl) carbamoyl)oxy)ethyl methacrylate)/citraconic anhydride	Polymeric micelles composed of PG and pH-responsive polymer	Low pH converts the polymer's citraconic amides to cationic primary amine, reverting the anionic nature of the polymer to cationic and inducing the release of positively charged chlorhexidine due to repulsion forces	[77]
	Doxycycline	Quaternary ammonium chitosan	Liposomes coated with quaternary ammonium chitosan	Acidic milieu protonates the residual amines of quaternary ammonium chitosan, destabilizing the particles and leading to drug release	[78]
	Farnesol	p(DMAEMA-co-BMA-co-PAA)	Polymeric micelles	Low pH values protonate diethylaminoethyl methacrylate (DEAEMA) and propylacrylic acid (PAA), and the resulting disturbance released encapsulated farnesol	[80]
	Ciprofloxacin and quorum sensing inhibitor	Hydrazine linker	Alginate nanoparticles	Acidic environment cleaved hydrazone bond between the polysaccharide and the quorum sensing inhibitor, releasing ciprofloxacin as well	[5]
	Polymer	poly(ethylene glycol)-COOH-polyethyleni- mine-2,3-dimethylmaleic anhydride	Carbon dots and polymer	Mildly acidic pH hydrolyses the amide in the polymer, reversing its charge from negative to positive and resulting in electrostatic repulsion between polymer and positively charged carbon dots, further converting the polymer into an antibacterial agent	[72]
	Vancomycin and 18β-glycyrrhetinic acid	Carboxilic group in the lipid and amine in polyallylamine hydrochloride	Lipid-polymer nanoparticles	At low pH the amine groups in polyallylamine hydrochloride and carboxylic group in oleic acid are protonated and repel each other, dispersing the system	[81]
Hyaluronidase	Gentamicin	Hyaluronic acid (HA)	Multilayer film of montmorillonite/HA-gentamicin	Hyaluronidase degrades HA and leads to gentamicin release	[82]
	Cateslytin (antimicrobial peptide)	Hyaluronic acid (HA)	Polysaccharide multilayer film of and chitosan	Degradation of HA in the presence of hyaluronidase for cateslytin release	[83]
Lipase	Triclosan	Ester link	Micelles with hydrophobic poly (β-amino ester) core and hydrophilic PEG shell	Ester linker is broken down by lipase and releases triclosan	[84]
	Cinnamaldehyde and ampicillin	Ester bond	Vertically aligned mesoporous silica coating loaded with ampicillin and cinnamaldehyde attached to nanovalves through an enzyme-sensitive linker	Lipase-triggered corelease of cinnamaldehyde and ampicillin; The system was also pH-responsive and the release profiles of the loaded compounds depend of the applied stimuli	[85]
	Triclosan	Polycaprolactone (PCL)	Polyurethane micelles with hydrophobic PCL corea and hydrophilic PEG shell	Degradation of polycaprolactone through lipase action; System is also pH sensitive	[86]
	Chlorhexidine	Caprolactam ring in Soluplus®	Polymeric micelles	Micelles of Soluplus® were enzyme-responsive for chlorhexidine release	[87]
Phosphatase/ Phosphoplipase	Vancomycin	Polyphosphoester	PEG nanogel	Cleavage of polyphosphoester leads to drug release from the system	[88]
Phospholipase A2	Doxycicline	Lipid	Liposomes with chitosan-modified gold nanoparticles	Phospholipid degradation by phospholipase A2 release drug due to destruction of membrane integrity	[89]
Gelatinase	Chloramphenicol	Gelatin	Gelatin nanoparticles in a microneedle patch	Gelatinase triggers the release of chloramphenicol in the biofilm	[90]
Hypoxia	Ciprofloxacin	Azo groups	Lactose-modified azocalix[4]arene	Reduction of azo groups by azoreductase leads to ciprofloxacin release after targeting of bacteria *via* the binding of lactose to the glycoproteins on the bacterial surface	[91]

pH-responsive DDS
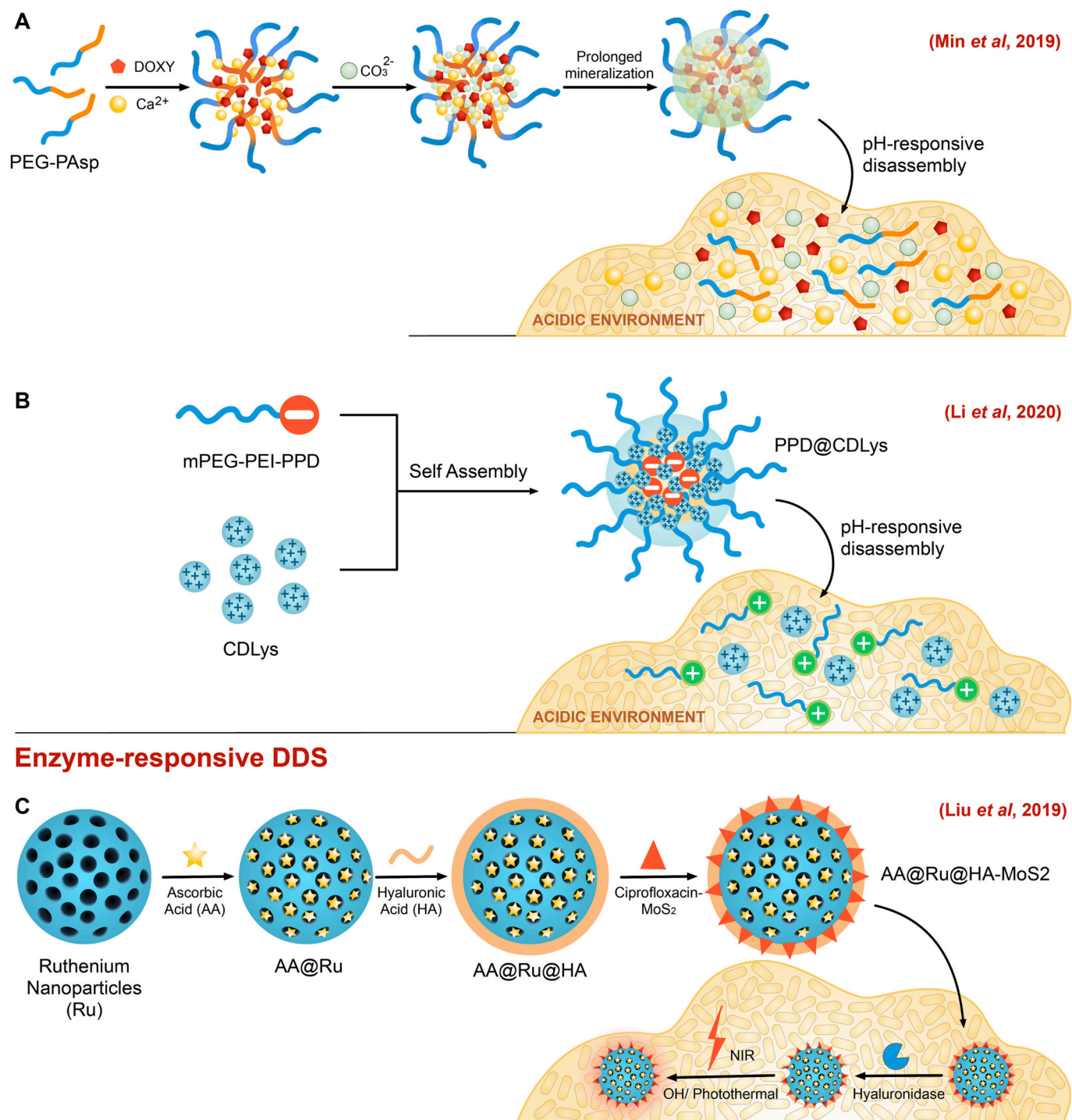
Fig. 2. Development of pH and enzyme responsive systems with enhanced biofilm penetration and activity. Adapted from [71]–[73].

observed for SSPM. Both carriers demonstrated a burst release of triclosan in the presence of lipase due to the enzymatic degradation of the hydrophobic group. Contrary to the single shelled system where no affinity or penetration was seen, MSPMs penetrated staphylococcal biofilms at pH 5.0. Reduction in metabolic activity was observed at low triclosan concentrations in the MSPM (compared to encapsulation in SSPM or alone) with evidence of Staphylococcal killing observed via bio-optical imaging.

To harness acid labile polymers that enhance surface binding at

relevant acidic environment, Horev and colleagues developed a self-assembled nanoparticulate system using acid labile 2-(dimethylamino) ethyl methacrylate (DMAEMA) and 2-propylacrylic acid (PAA) to expedite the release of farnesol and enhance binding to the dental surface at acidic pH conditions [80]. The nanoparticles comprised cationic poly (dimethylaminoethyl methacrylate) *coronas* and hydrophobic and pH responsive 2-(dimethylamino) ethyl methacrylate (DMAEMA), butyl methacrylate (BMA) and 2-propylacrylic acid (PAA) (p(DMAEMA)-b-p (DMAEMA-co-BMA-co-PAA)) cores. Destabilization of the nanoparticle

core at acidic pH led shorter half-life ($t_{1/2}$ = 7 h) at physiological pH compared to acidic pH ($t_{1/2}$ = 15 h) with approximately 75% drug release at pH 4.5 within 12 h. Compared to binding capacity of phosphate (50%) and alendronate (30%) functionalized micelles to hydroxyapatite, the protonated nanoparticle showed higher binding (67% binding) due to the increased protonation of the amine residues in p (DMAEMA). Caries scoring according to Larson's modification of Keyes system showed that topical treatment of *Streptococcus mutans* biofilms effectively reduced the number and severity of carious lesions *in vivo*. Colony counting assessment revealed that the nanoparticles achieved 80% reduction in colony forming units per biofilm dry weight whilst the free drug showed only a modest 20% reduction. Engineered alginate nanoparticles incorporating a pH-responsive linker between a quorum sensing inhibitor (QSI) and the backbone of alginate were also developed by Singh and colleagues [5]. The trigger was dependent on a hydrazine linker, used to connect the backbone of the polysaccharide and a QSI that targets the PqsR receptor. Charge to charge interactions between the alginate matrix and ciprofloxacin was employed as a strategy for drug loading against *P. aeruginosa* biofilms. It was reported that acidic conditions triggered the cleavage of the QSI from the alginate matrix alongside release of ciprofloxacin for synergistic antibacterial activities on pre-existing *P. aeruginosa* skin infection. Interestingly, testing the effect of the nanoparticles on a 2D keratinocyte infection model showed that the empty nanoparticles resulted in a significant reduction in the biofilm volume, average thickness, and surface area of the infection. Finally, *in vitro* assessment of the nanoparticle showed deep biofilm penetration of the nanoparticles which protected keratinocytes against *P. aeruginosa* infections. In another work developed by Li *et al*, the protonation of a shielding copolymer was exploited as a strategy to achieve pH triggered antibacterial response [72]. In their study, a carbon dot-based carrier was coated with poly(ethylene glycol)-COOH-polyethylenimine-2,3-dimethylmaleic anhydride. The polymer's protonation under mildly acidic conditions provoked a detachment from the positively charged carbon dots due to electrostatic repulsion. The disassemble of the carrier resulted in a unique synergistic antibacterial effect wherein the polymer had biocidal action and the carbon dots generated ROS. The system achieved a 60% inhibition of *S. aureus* biofilm formation, assessed through the measure of biofilm biomass, and destroyed preformed biofilms as seen through confocal laser scanning microscopy.

Hybrid nanoparticles were also used by Jaglal and colleagues as a pH responsive system for dual delivery of antimicrobial agents [81]. In this approach, an optimized lipid-polymer system was encapsulated with 18β-glycyrrhetinic acid (a pentacyclic triterpenoid) and vancomycin to achieve synergistic antibacterial effect. The pH-triggered protonation of the lipid core (composed of oleic acid) and polymeric shell induced cleavage of the ion pair bonds leading to a sustained and enhanced release of the antibiotic and 18β-glycyrrhetinic acid. The synergistic release of the antimicrobial agents led to a 16-fold increase in potency within 24 h compared to the use of vancomycin alone against planktonic MRSA. Surprisingly, enhanced potency was not observed against the susceptible strain wherein the formulation showed similar activity as bare vancomycin. Additionally, crystal violet assays demonstrated that although 69% elimination of MRSA biofilms was observed for the formulation, this was achieved using concentrations of 100 times greater than the minimum inhibitory concentrations which can have potential toxicity concerns.

4.2. Enzyme-responsive

The overexpression of specific enzymes at infection sites has provided researchers with strategies for the development of internal stimuli-responsive nanocarriers, typically focused on the cleavage of certain chemical bonds. Examples of reported enzymes used for these approaches include hyaluronidase, lipase, phospholipase, phosphatase, matrix metalloproteinase, gelatinase, glutamil endonuclease, penicillin G amidase and β-lactamase. A summary of different enzyme responsive systems can be found in Table 1.

Hyaluronidase-responsive systems are among the most reported systems for biofilm targeted treatment (Fig. 2). In this context, the team of Wang *et al* [82] developed a gentamicin-loaded multilayer film with antibacterial action triggered by hyaluronidase degradation. The multilayer films were based on the alternate self-assembly of montmorillonite/hyaluronic acid-gentamicin and revealed a controlled antibiotic release. This was dependent on the presence of hyaluronidase in the bacterial microenvironment through the degradation of the films in a top-to-down manner. This mode of action showed bactericidal properties and accounted for the prevention of bacterial attachment and preventing biofilm formation. Using confocal microscopy and colony counting methods, numerous living bacteria were observed for the control (87 ± 16 CFU/10^4 μm^2) whereas the film surface showed sporadically few living bacteria (<2 CFU/10^4 μm^2). A similar approach was tested against bacteria and fungi, where Cado *et al* developed a multilayer film functionalized with hyaluronic acid for hyaluronidase-responsive biofilm prevention, against both *Staphylococcus aureus* and *Candida albicans*. A cysteine residue was added to the C-terminal end of bovine cateslytin (an antibacterial and antifungal peptide) to graft it to hyaluronic acid, and the film was fabricated by depositing alternating layers of peptide-functionalized hyaluronic acid and chitosan on a surface. Such strategy showed a controlled release of the peptide upon exposure to these pathogens and fully inhibited the development of both species after 24 h as determined *via* the microdilution assay and colony counting [83].

Lipase-sensitive nanoparticles have been broadly reported as an antibacterial strategy resulting from its overexpression at infection sites. The mainly reported tactics focused on the cleavage of certain bonds as esters [84,85], fatty acid esters or anhydrides [92], polyesters such as polycaprolactone [86], aliphatic-aromatic polyesters (under specific conditions) [93] and polymers such as Soluplus® [87]. For example, Liu *et al* used an ester link to conjugate Triclosan to micelles formed by poly (ethylene glycol) (PEG)/poly(β-amino ester) (PEG-PAE) block copolymer that was degraded by bacterial lipases. PEGylation made the micelles biologically invisible, since they assumed a negative surface charged at physiological pH, and is thus suitable for blood stream transport of antimicrobials. Exposure of PAE moiety at acidic pH enabled self-targeting of bacteria and biofilm penetration after 2 h of exposure. Moreover, the system showed superior killing efficacy *in vitro* against multi-drug resistant strains of *S. aureus* and *E. coli* in comparison to the antibiotic solution, and was effective *in vivo* against sub-cutaneous MDR *S. aureus* infection in mice (using H&E staining) and *ex vivo* in human multi-species oral biofilms [84]. Against *Streptococci mutans*, confocal microscopy revealed that the triclosan micelles reduced biofilm viability to 4% upon 2 mins exposure whilst in *Streptococci mitis* 13% viability of the biofilms was observed. In another strategy reported by Wang *et al*, the deposition of nanovalves through an enzyme-sensible linkage on medical stainless steel was explored for dual pH and enzyme-responsive antibacterial activity. Following the coating of the material with vertically aligned mesoporous silica, the nanovalves (β-cyclodextrin functionalized with monopyridine) were immobilized to the coating (with a linker containing ester bonds) and both cinnamaldehyde and ampicillin were encapsulated into the silica coating. Since the system responded both to pH variation and enzyme presence, the release profile of the compounds differed depended on the trigger. Acidic pH microenvironments triggered the release of cinnamaldehyde alone, whereas under lipase action, both cinnalmaldehyde and vancomycin (through the cleavage of ester bonds) were released. [85]. Fluorescence microscopy images revealed that the carriers displayed outstanding anti-adherent performance and achieved 3.51-fold reduction in surviving *E. coli* adhesion compared to the control group. However, neither of the previously mentioned studies assessed antimicrobial activity against fungal biofilms that can also benefit from lipase-sensitive strategies.

The lipase-sensitive polymer polycaprolactone (PCL) was also used in a study by Su *et al* where three polyurethane micelles with a PEG hydrophilic shell and a PCL core were developed, the latter encapsulating triclosan. Lipase has been reported to degrade PCL and whilst all carriers showed triclosan release, different release profiles were reported, according to how tightly packed the PCL chains were in the different micelles. Under acidic conditions, the micelles showed effective biofilm penetration and antibacterial effect against *S. aureus* [86]. Moreover, the encapsulation of triclosan showed higher antimicrobial activity against planktonic bacteria than the free drug. Antibiofilm activities of the formulation revealed >90% destruction of *S. aureus* biofilms. Even though the authors consider the potential of one of the micelles for bacterial infection treatment, no *in vivo* assessment was conducted in this study.

In 2019, the team of Albayaty developed micelles based on Soluplus® and Solutol, at different mixing ratios, as lipases and esterases secreted by some microorganisms can degrade the caprolactam ring present in Soluplus®. Whilst Soluplus® micelles had an increase in chlorohexidine release upon lipase exposure, mixed micelles showed lower release in the presence of the enzyme. Regardless, crystal violet assays demonstrated a 2.4 and 2.1-log reduction in biomass for Soluplus® micelles and Soluplus-Solutol mixed micelles loaded chlorohexidine in MRSA, enhancing the penetration degree of chlorohexidine into the biofilms [87]. On the other hand, only 0.9 log reduction in CFU was observed for the free chlorhexidine. Phospholipase or phosphatase-responsive systems have been designed using phosphoesters and phospholipids for bacterial killing. In this context, Xiong *et al* created a macrophage-targeting nanogel with mannosyl ligands conjugated to poly(ethylene glycol) and polyphosphoester for degradation upon contact with bacteria-produced phosphatases or phospholipases. Such degradation led to the release of vancomycin, with antibacterial effect confirmed *in vivo* in zebrafish embryo model which demonstrated that the delivery system could responsively and effectively destroy bacteria [88]. A different approach was reported by Thamphiwatana and colleagues who were able to synthesize phospholipase A2-responsive liposomes, stabilized with chitosan-modified gold nanoparticles. With this synthesis, the team was able to prevent drug leakage and achieve controlled drug delivery upon exposure to the pure enzyme or *Helicobacter pylori*-secreted enzyme. Using Rhodamine B as a model drug, the authors showed increased release over time (that increased with higher bacterial concentrations), and a lower release profile when a phospholipase-A2 inhibitor was present. After liposomal loading with doxycycline, inhibition of bacterial growth was observed against *H. pylori*, which was reduced when an enzyme inhibitor was added to the culture, showing that a controlled release could be achieved [89]. However, the author's evaluation of formulation effectiveness was limited to the planktonic form of bacteria.

Alternative enzymes are gaining some attention as endogenous stimuli for triggered antibiofilm action. For instance, *Vibrio vulnificus* biofilms were treated with chloramphenicol encapsulated gelatinase-triggered nanoparticles that were loaded into a polyvinylpyrrolidone (PVP) microneedle patch. The team of Xu *et al* demonstrated a responsive drug release upon gelatinase exposure, with enhanced release of chloramphenicol when exposed to increasing enzyme concentrations. The application of the patch onto the biofilm resulted in physical disruption with drug diffusion observed through the biofilm matrix. Colony counts also revealed an enhanced antibiofilm effect of the patch with 63.2% reduction in colony forming units at 8 h in comparison to free chloramphenicol [90]. The authors reiterated the future applications of the patch as promising formulation to aid wound healing, however no *in vivo* studies were conducted.

4.3. Hypoxia-responsive

A hypoxic environment is another characteristic trait at a biofilm infection site. This feature is also present in tumors for example, and

hypoxia-triggered drug delivery systems have been developed for anti-tumor treatment [94]. However, limited studies have used this approach for antibacterial purposes, and the biofilm structure poses an additional challenge for their application. Nevertheless, the use of azo bonds in carrier design as a hypoxia-responsive function has been reported with promising *in vivo* results. In 2022, Li *et al* [91] developed a lactose-modified azocalix[4]arene loaded with ciprofloxacin and applied to diabetic multidrug-resistant *P. aeruginosa* infected wounds. In this work, a calix[4]arene core was loaded with ciprofloxacin and attached to the outer portion of the carrier through azo groups. The outer portion of the carrier was terminated with lactose as means of bacteria targeting (due to interactions between lactose and glycoproteins present at bacterial surface). Under hypoxic conditions, azo groups are reduced by azoredutases, freeing the antibiotic from the carrier's core. Triggered drug release was confirmed when reduced absorbance was observed after adding the chemical mimic of azoreductase, as well as an increase in fluorescence intensity (after loading the carrier with Rhodamine B). Moreover, drug release was assessed with confocal laser scanning microscopy, where bacterial treatment with different formulations revealed that the carrier loaded with a fluorescent dye displayed high fluorescence under hypoxic conditions, accompanied with the highest number of dead bacteria. Biofilm treatment with the carrier resulted in a reduction in biofilm thickness observed in confocal images, and up to 80% biofilm reduction (assessed *via* crystal violet staining assay). Moreover, *in vivo* infected wounds in diabetic mice showed quick wound closure after treatment with the loaded carrier. The plate counting method also revealed that almost no bacteria was present after 6 days.

5. Externally triggered DDS

5.1. Light-responsive

As reported above, there are several advantages in adopting the microenvironment of biofilms as a trigger for the antibacterial action of nanocarriers. Despite the benefits, challenges arise from variations in the microbial composition of biofilms. Accordingly, microbial composition of the biofilm plus the vast differences in the microenvironment where it forms (*e.g.*, skin, eye, mouth, vagina) ultimately impacts the performance of a formulation. To overcome such challenges, antibacterial nanocarriers can be designed to respond to an external trigger in a predictable manner. As an example, light is commonly used as an external stimulus to achieve spatiotemporal response, having different biomedical applications such as diagnostics, laser surgery, skin conditions and seasonal mood disorders [95]. Furthermore, the fabrication of light-activated nanocarriers is attractive since certain wavelengths, especially the near-infrared (NIR) window, allows for deep tissue penetration without significant damage to healthy surroundings [96,97]. The synthesis of a light-responsive nanocarrier with antibiofilm action can therefore be a suitable approach for on-demand antibacterial action for clinical applications. Examples are summarized in Table 2 and representative studies are illustrated in Fig. 3.

5.1.1. Photothermal therapy

Within the scope of light-triggered carriers, photothermal therapy (PTT) is a concept applicable to nanomaterials with the ability to convert photonic energy (within the spectral range of 650–900 nm) into heat. The subsequent damage to the biofilm is due to local hyperthermia generated upon radiation and mediated by the strong absorption properties of the nanocarriers. Moreover, the heat generated from PTT can unleash certain chemical reactions. Examples include the destruction of non-covalent interactions between a nanoparticle and active molecules (such as an antibiotic) [104], enzyme activation [105], nitric oxide release (using NO donors such as N-Diazeniumdiolates and S-nitrosothiols/S-nitrosoglutathione [103] or even the induction of movement [98]. A myriad of materials can be employed for PTT, such as the noble

Table 2

Light-triggered drug delivery systems.

| Trigger	Strategy	Active compound	Core material	Stimuli responsive interaction/System	Purpose	Reference
Light	Photothermal therapy	Daptomycin	Gold	Non-covalent bond between carrier and antibiotic	Increase in temperature destroyed non-covalent interactions between antibiotic and carrier	[115]
		Bromelain (protease)	Gold	Conjugation between gold nanorods and cysteine residue in the protease (using Au—S chemistry)	Increase in temperature made the protease reach its optimal temperature reaction (with consequent enterotoxin destruction)	[105]
		Hydrogen	Pd	Interaction forces between H_2 and Pd atom	Increase in temperature destroyed interaction forces between carrier and hydrogen	[116]
		Gold nanoparticles + vancomycin	Mesoporous silica	Vancomycin loaded SiO_2 shells with gold nanoparticles embedded in the inner face	Increase in temperature induced the motion of the carrier to deeper biofilm layers	[98]
		Penicillin	MoS_2	Non-covalent (hydrophobic adsorption)	Increase in temperature led to antibiotic release	[104]
		Azythromycin/ Tobramycin	Carbon	Hydrogen bonds (between C=O groups of carbon quantum dots and OH of azithromycin or NH of tobramycin)	Loaded carbon quantum dots were incorporated into PLGA NPs; The temperature increases to a value equal or above glass transition temperature of PLGA and induced a phase transition of the carrier with consequent antibiotic release	[99]
		S-nitrosothiol (NO donor)	Graphene	–	Temperature increase breaks S-NO bonds for NO release	[128]
		Tobramycin	Cyanine dye (Cypate)	Encapsulation into liposomes	Temperature increase leads to enhanced membrane permeability of liposomes and release of encapsulated drug	[130]
		N-diazeniumdiolate (NONOate)	Polydopamine-coated iron oxide	Conjugation between secondary amine groups of a dendrimer and NONOate	Temperature increase causes the release of NO	[100]
		Vancomycin	Tungsten sulfide quantum dots	Encapsulation into liposomes	Temperature increase disrupts the liposome and leads to vancomycin release	[132]
	Photodynamic therapy	L-arginine-rich peptide dendrimers (NO release)	Chlorine e6	Loading of chlorin e6 in the self-assembled dendritic peptides	H_2O_2 generated oxidized L-arg-rich dendritic peptide to NO and L-citrulline	[101]
		CORM-401 (CO release)	Chlorine e6	Self-assemble of a fluorinated amphiphilic dendritic peptide	H_2O_2 generated oxidized CORM-401 for CO release	[102]
		Thymol	Toluidine blue O	Self-assemble of toluidine blue O grafted chitosan and poly(propylene sulfide) (PPS)	ROS generated oxidized hydrophobic sulfide in PPS to hydrophilic sulfoxide or sulfone and enabled thymol release	[146]
	Photothermal and photodynamic therapy	L-arginine	Indocyanine green and mesoporous polydopamine	Covalent or electrostatic interaction (functionalization of mesoporous polydopamine nanoparticles through dihydroxyindole/ indolequinone groups with L-arg); π- π stacking of ICG (due to aromatic rings and mesoporous NP structure)	Increase in temperature led to the dye's release; ROS generated by the dye led to NO release from L-arg	[103]

metals (gold and silver), carbon (and, by extension, graphene), transition metal dichalcogenide nanostructures (WS_2, MoS_2), metal-oxide nanoparticles and nanoscale coordination compounds (Prussian blue nanoparticles) [96,106]–[108]. The application of these materials against biofilm infections has benefits for "on-demand" release of therapeutic cargos and other antibacterial compounds. While current literature widely explores PTT for antitumor purposes, growing evidence is showing their efficacy for the treatment of planktonic and biofilms infections, further detailed in the following sections. It is worth noticing that many other relevant studies have been conducted in planktonic bacteria [109] and even *in vivo* [110,111], however were not included in this review as they did not assess antibiofilm effect directly.

Metals. Noble metals have been widely employed in designing nanocarriers for PTT due to the ease of heat generation when irradiated with NIR lasers. The oscillation of valence electrons on their surface accounts for the light-to-heat conversion efficiency [112] wherein the irradiation causes a thermal relaxation and induces a temperature increase.

Moreover, because the conditions during synthesis impact the absorption peak, it is possible to choose which wavelength the carrier will absorb [113], making many metals an optimal choice.

Among the different metals available for PTT, gold is one of the most favoured owing to its strong surface plasmon resonance properties [114]. Moreover, different morphologies for gold nanoparticles have been reported in the literature, including nanospheres, nanorods, nanocages, nanoflowers and nanoshells [114], supporting the versatility of this metal. Additionally, gold-based nanoparticles can be coupled with active molecules for on-demand release. As an example, antibiotics are frequently loaded in smart carriers since their thermally triggered release can have a synergistic effect with PTT itself. In a recent work by Meeker *et al* [115], daptomycin was incorporated into gold nanocages by noncovalent interactions and coated with polydopamine. For selectivity purposes, the carrier was conjugated to an antibody targeting staphylococcal protein A, a protein commonly found on the surface of *S. aureus* species. The irradiation of the targeted area provoked a temperature increase that destroyed the noncovalent interactions between daptomycin and the carrier, thus promoting drug release. Bacteria
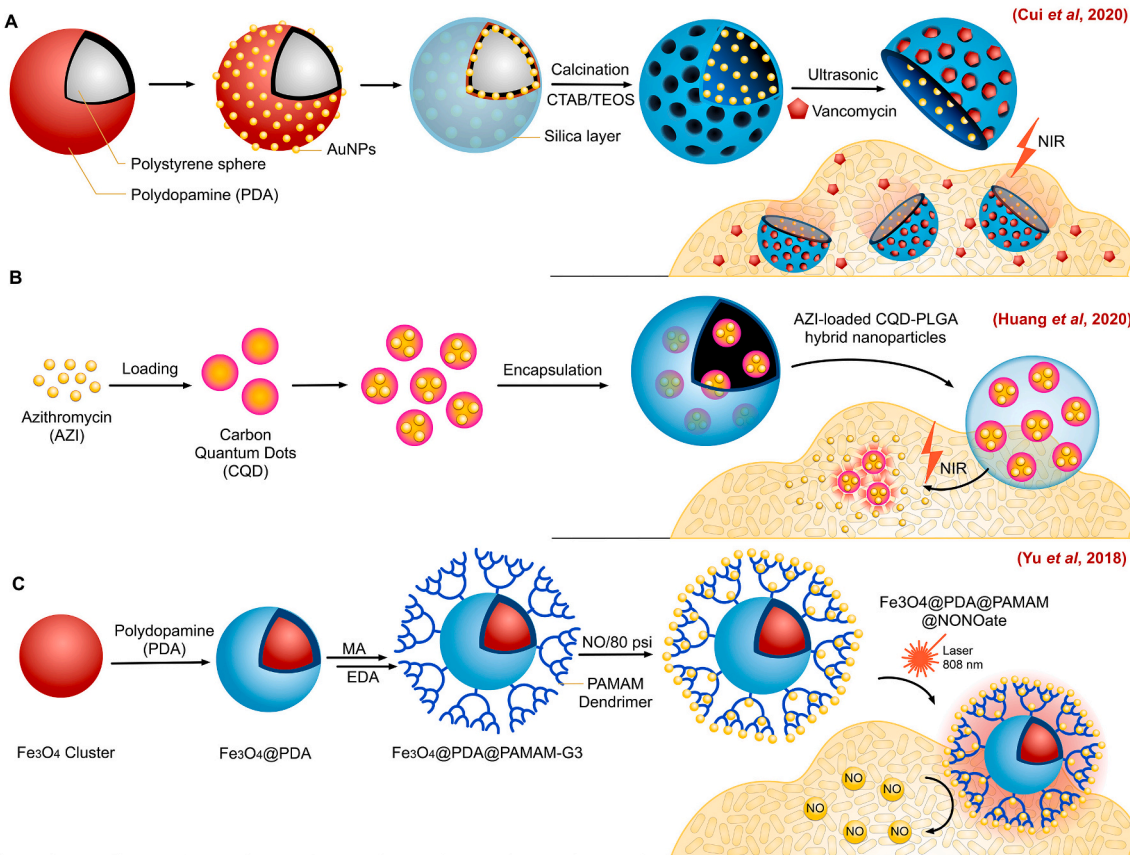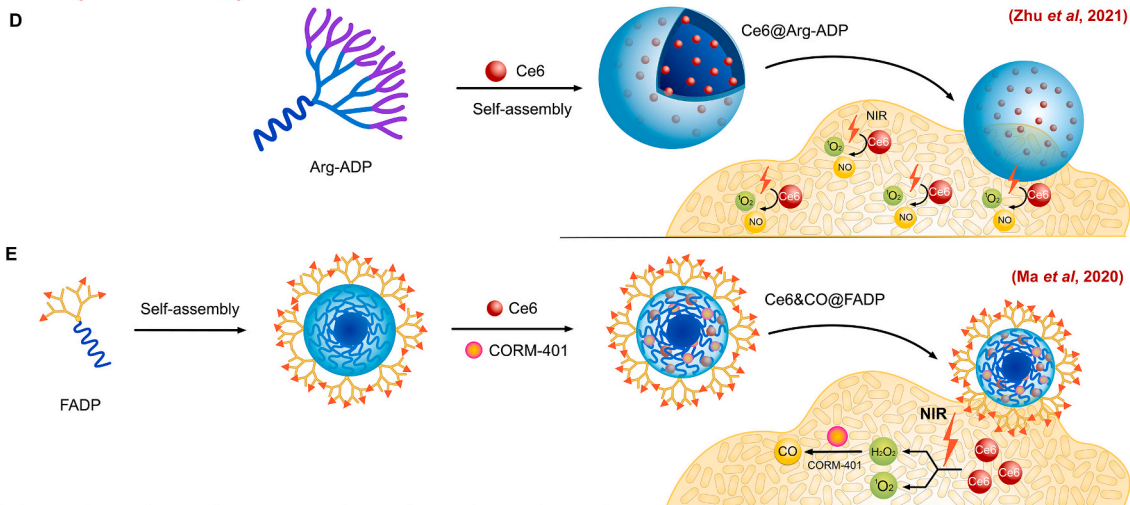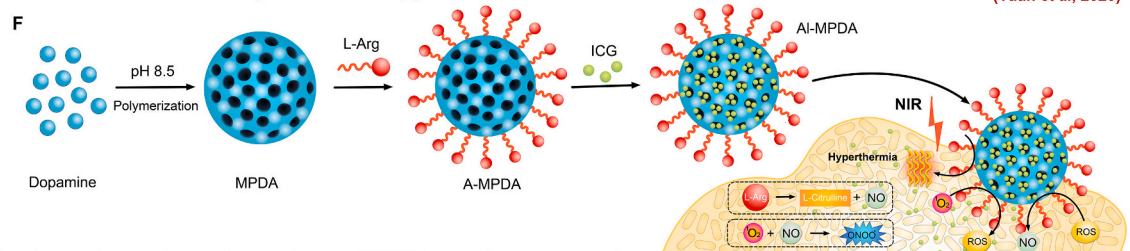
Fig. 3. Development of nanomaterials for photothermal and photodynamic therapy. Adapted from [98]–[103].

viability assessment *via* colony counting revealed no recovery of viable bacteria at either the immediate or 24 h time point in MRSA biofilms which strongly supports the synergistic effects of PT killing and daptomycin potency.

Even though most studies focus on antibiotic release, some projects use heat to trigger the activity of proteases towards protein destruction. For example, the team of Li et al. [105] developed protease-conjugated gold nanorods. The protease bromelain has its optimal reaction temperature at 50 °C, a value well above physiological temperature but achievable *via* NIR irradiation of the gold nanocarriers. After reaching this temperature, the carrier-conjugated protease was able to destroy enterotoxin, an exotoxin secreted by *S. aureus*. The combination of the protease activity with the thermal effect from the particles resulted in a synergistic effect that culminated with the destruction of bacterial cells, biofilms and exotoxins. A different strategy was used by Yu and colleagues [116], where cubic-shaped Pd carriers were loaded with hydrogen. In this work, hydrogen was released from the cubic lattice through laser irradiation in a power-dependent manner and showed antibacterial and wound healing properties. Additionally, the system seemed to increase the amount of ROS, causing DNA damage and the upregulation of certain genes involved in DNA repair (recA) and encoding for pro-oxidative enzymes (*dmpI, narJ, nark*). Effective biofilm eradication was observed *via* CV measurements and confocal microscopy was confirmed *in vitro,* and *in vivo* studies showed antibacterial and wound-healing effects on *S. aureus* infected wounds.

Other ingenious approaches have been designed to take advantage of heat generation. One published strategy promote a deeper penetration into the biofilm matrix inducing movement of the nanocarrier. A study developed by Cui *et al* [98] reported NIR-driven nanoswimmers consisting of mesoporous silica half-shells asymmetrically functionalized with gold nanoparticles. The placement of gold nanoparticles on the interior portion of the shell resulted in a heat-driven motion, propelling the carrier to evenly spread throughout the biofilm. The authors loaded vancomycin into the carriers which was released only upon laser irradiation. The system demonstrated a thermally triggered motion, antibiotic release and photothermal effect with a 5-fold log reduction in biofilm colonies as demonstrated *via* confocal and colony counting techniques. This culminated into improved treatment of biofilm infections *in vivo* without obvious signs of toxicity.

Transition metal dichalcogenides are two-dimensional materials with unique properties that allow for their use in biosensors, drug delivery, imaging and even tissue engineering [117]. They have gained attention for PTT as a result of their tuneable bandgaps, strong spin-orbit coupling, thermal conversion, optical efficiency, cytocompatibility, ease of surface modification, stability and low cost [118,119]. Characterized by the general formula MX_2 (where M stands for transition metals from group 4 to 10 in the periodic table and the X represents chalcogen elements (namely S, Se and Te)) [120], transition metal dichalcogenides are typically made of two layers of a chalcogen atoms separated by a layer of transition metal atoms. Some examples include MoS_2, WS_2, TiS_2, ReS_2, $MoSe_2$, WSe_2 and TaS_2. These compounds are predominantly used for cancer therapy, however some approaches to target bacteria and biofilms have gained popularity. In this context, Zhang *et al* [104] developed a MoS_2 nanosheet loaded with penicillin through non-covalent adsorption. Drug release was dependent on the laser in a power-dependent manner, wherein higher power resulted in faster release profiles. Using colony counting assays and confocal microscopy, the combination of photothermal and chemotherapy exhibited >70% reduction in *S. aureus* and *E. coli* biofilms in comparison to the free drug. Even though neither the loaded nor unloaded nanosheets exhibited toxicity against fibroblasts, the study did not evaluate the toxicity effects of the carriers under NIR irradiation.

Other compounds. While metals and transition metal dichalcogenides represent the majority of materials employed for PTT, other molecules

and compounds have attracted attention for antibacterial and antitumor therapy. Some broad examples include carbon and graphene [121], dyes (such as FDA approved indocyanine green and IR780) [122], conductive polymers (polypyrrole and poly-(3,4-ethylenedioxythiophene):poly(4-styrenesulfonate) (PEDOT:PSS)) [110,123], magnetic Fe_3O_4 nanomaterials [124], tungsten oxide [125], black phosphorus [111], polydopamine [126] and coordination compounds (*e.g.* Prussian blue nanoparticles) [107].

Carbon-based nanoparticles are an example of inorganic materials with NIR-responsive properties [127]. The optical, electrical and mechanical properties of carbon-based carriers make them attractive tools for antitumor and antibacterial therapy using nanotechnology [96]. In a recent study by Huang *et al* [99], azithromycin and tobramycin were separately loaded in carbon quantum dots. Thereafter, the carrier was incorporated into PLGA nanoparticles using a microfluidic method. This FDA-approved polymer is biocompatible, stable, and able to protect loaded drugs against degradation, yet is unable to provide on-demand drug release when used alone. By incorporating carbon quantum dots into PLGA, the NIR-triggered antibiotic release and photothermal effect acted synergistically to eradicate *P. aeruginosa* biofilm as imaged with confocal microscopy. In another work conducted by Zhao *et al* [128], a nitric oxide (NO) donor was bound to a graphene platform. In this study, boronic acid was additionally used to selectively bind to bacteria, since it has been previously described to target LPS. Following irradiation at 808 nm, the hyperthermia generated by the graphene platform triggered NO release, achieving an on-demand synergistic effect between NO and PTT thereby inducing bacterial cell membrane destruction and anti-biofilm effect. The efficacy of the system against MDR *P. aeruginosa* revealed 80% elimination of biomass *via* CV staining.

Photothermal therapy can also benefit from the use of certain dyes. As an example, IR-780 iodide is a NIR fluorescent lipophilic dye with stable fluorescence that can be loaded into hydrophobic carriers [129]. Another dye with photothermal activity is cyanine dye (cypate), used by Zhao *et al* as a photosensitizer for an antibiotic-loaded thermosensitive liposome [130]. The positively charged liposomes had a temperature-dependent membrane permeability, allowing for controlled drug release upon temperature increase. The photothermal effect generated by cypate led to the melting of the liposomes, releasing 80% of the loaded tobramycin. Moreover, the team discovered that this treatment could stimulate the expression of a bcl2-associated athanogene 3 to prevent normal tissue from thermal damage, allying PTT, antibiotic treatment, and wound healing promotion. Furthermore, CV staining and SEM images demonstrated a 7 to 8-fold increase in biofilm removal in comparison to the free tobramycin following treatment with the formulation and NIR irradiations A maximum dispersal rate of 79.8% was observed in PAO1 biofilms.

Likewise, polydopamine (PDA) has started to attract researchers' attention for photothermal purposes. The surface of PDA NPs also enables the adsorption of different molecules *via* π-π stacking and/or hydrogen bonding, allowing the particles to act as drug carriers for NIR triggered drug release [131]. In this context, Yu *et al* [100] envisioned a strategy to achieve synergistic effect between PTT and NO release, allied with bacterial removal. In this work, iron oxide nanoparticles were used as the carrier's core, and coated with polydopamine to achieve a photothermal effect. The surface was then functionalized with quaternary ammonium-modified poly(amidomine) dendrimers that reacted with NO to generate N-diazeniumdiolate (NONOate). This NO-donor material induced damage to the bacterial membrane of *S. aureus* and *P. aeruginosa* and led to biofilm eradication using CV staining. Even though the carrier alone was able to reduce bacterial viability to 60% in both pathogens, the combination of the nanoparticle with laser effectively reduced the bacterial viability in a concentration-dependent manner. Similar results were obtained for biofilm eradication. Furthermore, the study showed that it was possible to separate bacteria from a bacterial suspension after the application of an external magnet due to the superparamagnetic properties of iron oxide nanoparticles. Given that bacteria can spread

through the bloodstream after biofilm destruction, the property of separating bacteria is fairly attractive for antibacterial purposes to prevent systemic infection. Another work also combined antibiotic release with PTT as an antibacterial strategy. Xu and colleagues [132] developed a liposome-based photon-responsive drug-delivery system for combined chemodynamic therapy, photothermal therapy and pharmacological action. For this purpose, tungsten sulfide quantum dots (WS$_2$QDs) and vancomycin were loaded into the liposome to synthesize a temperature-sensitive carrier. This work combined chemodynamic therapy (the effect that nanozymes can have to mimic peroxidase activity and convert H$_2$O$_2$ into free radicals) with other antibacterial approaches to strengthen antibacterial effect. Moreover, the study assessed the level of glutathione oxidation of the system since glutathione is known to be present at infection sites and reduce chemodynamic effect. After irradiation, the liposomes were disrupted by the heat generated by tungsten sulfide quantum dots, resulting in the antibiotic release. Crystal violet staining revealed that the irradiated liposomes enabled >80% reduction in relative *S. aureus* biofilm biomass and *in vivo* studies showed over 80% reduction in relative bacterial viability in *S. aureus* infected abscesses in mice without signs of major toxicity.

5.1.2. Photodynamic therapy

In addition to photothermal applications, light is fairly used in other treatments modalities. Accordingly, many articles have reported its use in photodynamic therapy (PDT) as an antitumor approach, and the concept of antimicrobial PDT has also showed successful results. Its mechanism of action relies on the presence of oxygen and a photosensitizer to generate molecules that are harmful to bacteria. Generally, the photosensitizer is activated (through the energy coming from a light source), reaching its singlet excited state (PS*) [133]. Subsequently, through intersystem crossing, the PS molecule reaches its lowest-energy excited triple state and transfers energy to molecular oxygen (O$_2$) through two mechanisms, generating either reactive oxygen species (ROS) (type-I mechanism) or reactive singlet oxygen (^{1}O$_2$) (type-II mechanism) [134]. Such compounds lead to oxidative stress in bacterial cells [135] with DNA [136], lipid [137] and protein destruction [138]. Consequently, the unspecific and broad-spectrum mechanism of action of PDT does not induce bacterial resistance, a feature that stands out as one of the main advantages of this strategy [136]. Even though some limitations are inherent to PDT (related with low efficacy against biofilms and poor efficiency in animal models [136]), the strategy has become promising with proven efficacy against different microorganisms [139]. Similarly, to the studies reported for PTT, smart carriers can be designed using the photosensitizer's reaction to light as a trigger to release antibacterial molecules. The difference relies on the fact that PDT uses the ROS generation to oxidize the carrier and promote the controlled release of other compounds. Some examples include phenotiazinium dyes (such as methylene blue, toluidine blue, rose bengal), natural compounds (as curcumin and hypericin), tetrapyrrole structures (porphyrin, phthalocyanines, chlorine) and nano structures (fullerenes and titanium dioxide) [140].

Among different photosensitizers, chlorin e6 (Ce6) has been fairly used for PDT alone or in combination with other antibacterial strategies. One of the main approaches is to combine PDT with gas therapy, such as nitric oxide (NO), for simultaneous antibacterial action generated both by ROS and NO molecules. NO is an endogenous molecule that promotes wound healing through vasodilation, as well as myofibroblasts and collagen production, stimulating wound healing [141,142]. However, NO is also capable of inducing lipid peroxidation, DNA cleavage and protein dysfunction, and is therefore viewed as an antibacterial agent with a broad spectrum of action [143,144]. For these reasons, it has been employed by Zhu *et al* [101] in combination with PDT for biofilm eradication. The team developed a PDT-driven NO generation system using L-Arg-rich amphiphilic dendritic peptide as a carrier. L-Arg is a biocompatible NO donor, yet its encapsulation poses a challenge for development of nanocarriers. This led the team to envision a

macromolecule-based system with the ability to load L-Arg and achieve precise regulation of NO release, based on a new type of biomedical polymer – peptide dendrimers. Specifically, L-arginine-rich peptide dendrimers with guanidine groups (reported to provide biocompatibility and effective cell penetration). Since L-Arg-rich amphiphilic dendritic peptide (Arg-ADP) generates NO in the presence of ROS and inducible NO synthase, the team hypothesized it could be used as an NO donor. In summary, L-arg-rich amphiphilic dendritic peptide were loaded with Ce6 for synergistic antibacterial effect between PDT and PDT-driven NO release. When irradiated with a 665 nm laser, Ce6 resulted in the generation of ^{1}O$_2$ and H$_2$O$_2$. Afterwards, H$_2$O$_2$ oxidizes Arg-ADP to NO and L-citrulline, and the combination of ^{1}O$_2$ and the reactive by-products of NO resulted in synergistic antibacterial effect as well as biofilm eradication. Crystal violet assays demonstrated 90% ablation in MRSA biofilms for the carrier. Furthermore, confocal microscopy and SEM imaging revealed a nearly complete destruction of the cell membranes in the biofilms as evidenced by the extremely strong red fluorescence and severely deformed or totally lysed MRSA cells respectively. The study of *in vivo* efficacy was assessed in subcutaneous abscesses, where the carrier also proved to effectively remove bacteria from abscess site and generate NO to promote wound healing. Similarly, carbon monoxide was used by Ma *et al* [102] to enhance the antibiofilm effect of PDT. In this study, a fluorinated amphiphilic dendritic peptide (FADP) was loaded with Ce6 and CORM-401. The latter is a CO-releasing molecule, whose release is dependent on the presence of oxidants such as H$_2$O$_2$ [145] generated after Ce6 irradiation. Additionally, the fluorinated carrier was expected to show enhanced penetration into biofilms and cellular internalization due to high electronegativity, hydrophobicity, and membrane permeability of fluorine. In general, the carrier provided an efficient antibacterial feature and resulted in the ablation of biofilms, with an on-demand release of CO. Crystal violet staining revealed 92% and 90% inhibition of *S. aureus* and *E. coli* biofilms *in vitro* alongside 95% eradication of *E. coli* biofilms. In *S. aureus* infected skin tissues, bacteria colony counts showed 9-fold lower bacteria count after treatment. The formulation also demonstrated excellent biofilm eradication (*via* H&E staining) as no *S. aureus* colonies were recovered on the wounds after 3 days.

A different approach was pursued by Wang *et al* [146], where gas therapy was replaced by the use the essential oil thymol. Essential oils possess inherent hydrophobicity that allows them to disrupt the bacterial cell membrane. However, they are challenged by insolubility and instability in hydrophilic environments, often leading to the need to be encapsulated in nanocarriers. Therefore, chitosan micelles were loaded with thymol for controlled antibacterial action. The micelles encapsulated the photosensitizing agent toluidine blue O (TBO), and were prepared *via* self-assembly of toluidine blue O grafted chitosan and poly (propylene sulphide) (PPS). The cationic nature of chitosan allows the micelles to bind to the biofilm and PPS was used as its hydrophobicity can be changed in the presence of ROS. When these species are present, the hydrophobic sulfide in PPS can be oxidized to hydrophilic sulfoxide or sulfone, a change that enables thymol release. The release of thymol combined with photodynamic therapy (10 mins irradiation) itself led to more than a 60% reduction in biofilms (<0.4 relative biofilm value was achieved) when assessed with CV staining in *S. aureus* biofilms. Confocal microscopy and SEM imaging also showed only scanty pieces of bacteria colonies and no recognizable intact structures of *S. aureus* biofilms.

5.1.3. Photothermal and photodynamic therapy

As summarized in previous sections, both PTD and PTT have shown great potential for on-demand antibiofilm action, and the combination of both strategies has also shown promising results. In 2020, Yuan *et al* [103] used L-arginine (L-arg) as NO donor, a molecule capable of reacting with ROS to generate reactive peroxynitrite (ONOO-), compounds, with the ability to cause lipid peroxidation. The carrier's core was composed of mesoporous polydopamine (MPDA) modified with L-arg and indocyanine green. Since ICG was loaded *via* π-π stacking, the

effect of temperature increment on MPDA upon irradiation led to the dye's release. In turn, ICG produced ROS under the same external trigger leading to NO generation *via* L-arg catalysis. The synergistic effect of this combination treatment was revealed *via* colony counting of detached *S. aureus* biofilms which showcased a 99% reduction in established biofilms. Crystal violet staining revealed a biomass reduction of 80% compared to the control group. Strikingly, with 2 mins NIR irradiation, the carrier showed 61.7% reduction in biofilm survival thereby demonstrating the effectiveness of the formulation under short-term NIR exposure. *In vivo* studies also corroborated the antibiofilm effect of the system without major toxicity signs. Even though the studies on the use of PDT and PTT simultaneously for combination therapy against biofilms are limited, the opportunities it bears for an enhanced antibiofilm activity are exciting.

5.2. Temperature-responsive and magnetic field-responsive

The use of temperature as trigger for smart antibiofilm action has been used and described in previous sections, especially as the basis for photothermal therapy, where its increase typically destroys weak interactions between a carrier and a loaded drug, to enhance the release of the drug. The temperature value is typically above physiological temperature and results from conversion of NIR-light to heat. However, body temperature on its own can act as a stimulus for controlled drug delivery, usually related to the physicochemical characteristics of the formulation (Table 3). Formulations whose properties change at physiological temperature demonstrate how the body temperature can influence drug delivery. In this context, a study was conducted by Overstreet *et al* [147], where temperature-responsive polymeric gels were loaded with tobramycin and vancomycin. These formulations were based on an aqueous solution of the polymer poly(*N*-isopropylacrylamide-*co*-dimethylbutyrolactone acrylate-*co*-Jeffamine M-1000 acrylamide) (PNDJ), whose lower critical solution temperature is below physiological temperature. Such characteristic implies that the aqueous solution changes to a gel upon heating to body temperature. Afterwards, hydrolysis-based changes in lactone moieties of a repeat unit in the polymer lead to the increase of the lower critical solution temperature. When this value becomes higher than physiological temperature, the polymer dissolves and drug release is enabled. Interestingly, the authors found that the release was faster *in vivo* than *in vitro* and that drug delivery was site-dependent rather than formulation dependent. Despite the fact that the study had some limitations, the formulations appear to be a feasible approach for antibiofilm purposes

as the antibiotic concentrations were in the order of the minimum biofilm eradication concentration and were sustained for 24-72 h.

Other gels with similar thermoreversible traits have been synthesized. For example, a poloxamer hydrogel has been designed for antibacterial effect against *E. faecalis* by Liu and colleagues [148] (Fig. 4). The silver nanoparticle-loaded gel was liquid at room temperature but acquired a gel texture at 30 °C (due to the ability of poloxamers to self-assemble into micelles) and showed the release of nanoparticles over the course of 9 days. Confocal and SEM images were used to assess the performance of the formulations. A dose dependent reduction in *E. faecalis* was observed and the highest reduction (>84.88%) in bacterial colonies seen after 9 days for the highest dose (32 μg/mL) of the formulation. Both studies focused on biofilm infections in the human body, yet this temperature-responsive strategy can also be envisioned for other biomedical applications such as protection against infections in medical devices. As such, Choi and colleagues [149] developed levofloxacin-loaded polymeric brushes as functional coating for titanium implants. The thermo-responsive 400 nm poly(di(ethylene glycol) methyl ether methacrylate) coating released levofloxacin in a temperature and brush thickness-dependent manner with concomitant antimicrobial effects *in vivo* and *in vitro*. Quantitative assessment of biofilm performance was assessed using luminescent imaging and they revealed >99.9% reduction in luminescence intensity and SEM verified the antifouling effect of the brushes on the titanium plates. Taken together, these studies focused on using the lower critical solution temperature property of certain polymers and highlight how body temperature can be used as a smart trigger for antibiofilm action with different biomedical applications.

The application of an external magnetic field combined with magnetic particles has been explored in the last years for therapeutic and diagnostic biomedical applications[150]. One advantage of combining magnetic nanoparticles with a magnetic field is the possibility of generating a local magnetically triggered increase in temperature, a desired feature for targeted biofilm eradication. The temperature increase results from the alternating magnetic field of action on the particles, reorienting their magnetic moment through Néel mechanism or Brownian rotation [150]. For antibiofilm purposes, the strategies include magnetically-induced hyperthermia combined with thermoresponsive polymers [151], antibiotic release [152] or penetration enhancement of harmful compounds [153] (Table 3). Similar to some strategies presented above, the use of this external trigger is often coupled with the release of an antibacterial compound. As an example, Hua *et al* [152] encapsulated ciprofloxacin in PLGA magnetic particles

Table 3
Temperature and magnetically triggered drug delivery systems.

| Trigger	Active Compound	Function	System	Purpose	Ref
Temperature	Tobramycin and vancomycin	Polymer poly(N-isopropylacrylamide-co-dimethylbutyrolactone acrylate-co-Jeffamine M-1000 acrylamide) (PNDJ)	Gel	Gel formation upon heating of the solution to physiological temperature with subsequent dissolution and drug release (due to changes in the lower critical solution temperature values)	[147]
	Silver nanoparticles	Poloxamer	Gel	Gel formation upon heating of the solution to physiological temperature due to the ability of poloxamers to form micelles	[148]
	Levofloxacin	Polymer poly(di(ethylene glycol) methyl ether methacrylate) (PDEGMA)	Brushes	The brushes release the antibiotic after reaching temperature values above lower critical solution temperature	[149]
Magnetic	Ciprofloxacin	PLGA Magnetic NPs	–	Oscillating magnetic field led to drug release due to mechanical poration and/or thermal energy generation	[152]
	Cetyltrimethylammonium bromide (CTAB)	Iron oxide	–	Rotating magnetic field was used to transport CTAB through the biofilm matrix in vertical and horizontal movements	[153]
	D-aminoacids	Iron oxide NP	Hydrogel (glycol chitin)	Exposure to an alternating current magnetic field leads to heat generation by iron oxide NPs and changes the thermoresponsive polymer from a solution to a gel	[151]
	Glucose oxidase	Magnetic NPs (Fe$_3$O$_4$)	–	Magnetic field induces movement of the nanoparticles and leads to ROS generation and nutrient depletion through the action of the enzyme	[154]

Temperature-sensitive DDS
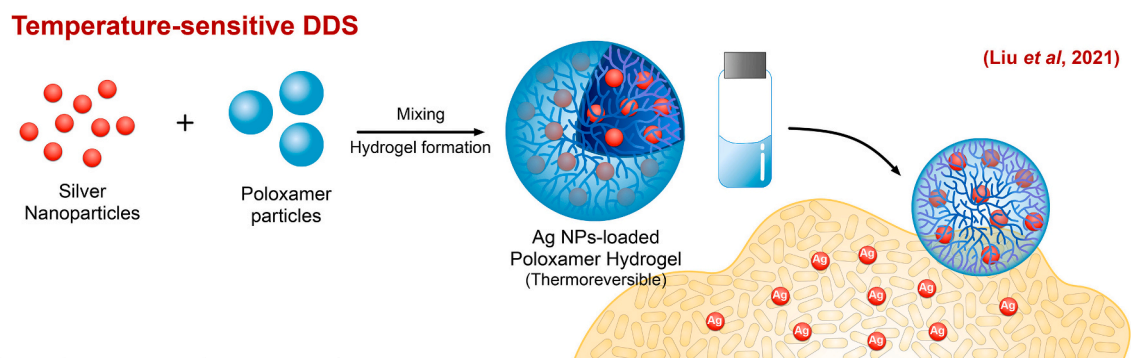
Fig. 4. Development of a formulation with temperature-sensitive properties against biofilms. Adapted from [148].

and used either sonication or homogenization for the synthesis of nano and microparticles, respectively. Despite the different carriers' sizes (221 nm for nanoparticles and 1.5 μm for microparticles), both particles increased drug release after being subjected to an external oscillating magnetic field. Moreover, the microparticles revealed surface cracks after magnetic field exposure, which might suggest mechanical poration caused by activated magnetic nanoparticles, explaining the reason for a higher drug release in comparison to the control within 4 h. Such surface effect was not observed for the nanoparticles, and even though both released similar drug percentages within 6 h of magnetic field exposure, the microparticles displayed a higher drug release for the first 15 days of the experiment. Interestingly, the researchers assessed the magnetic responsiveness of the system by subjecting them to a "turn-on and -off switch" of the magnetic field experiment and measured drug release. A significant increase was observed during the "on" periods, in comparison to a low drug release during the "off" phases, confirming the responsiveness of the system to the stimuli. Using XTT assays to assess the metabolic activity of the biofilms, both formulations showed similar potencies resulting in 33.5% and 33.3% inhibition of *P. aeruginosa* biofilms as a result of the magnetically triggered antibiotic release. In another work by Nickel *et al* [153], the biocide cetyl-trimethylammonium bromide (CTAB) was loaded into iron oxide nanoparticles. Since the biocide alone has poor penetration into biofilms, the loaded particles were subjected to a rotating magnetic field to induce vertical and horizontal movement of the carrier inside the matrix. Such strategy allowed the diffusion of the compound through the generated holes and thus aided its effectiveness in biofilm destruction. Furthermore, the team assessed how different shapes of the carrier could influence its loading ability, using iron oleate decomposition to synthesize spheres, cubes and tetrapods. The method resulted in an oleic

acid coating of the carrier's surface, and the loading was proportional to the length-to-volume ratio (increased load for particles with sharp edges). The tetrapods had the highest loaded percentage (around 10%), followed by the cubes (around 4.5%) and spheres showed the lowest (around 0.3%). Using CV staining, colony counting, SEM and confocal microscopy, both the cubes and tetrapods fully eradicated (14.19 $\log_{10}$ reduction) MRSA biofilms, with a lower biofilm reduction induced by the spheres (7.3 $\log_{10}$ reduction). The team correlated the efficacy with the enhanced biocide transport into the matrix (due to higher biocide loading). Both articles showed how different carriers can load a compound for biofilm destruction and exert their action after magnetic stimuli.

A different approach was reported in 2018, where Abenojar and colleagues developed a magnetic hydrogel nanocomposite to eradicate *S. aureus* biofilms [151] (Fig. 5). Since amino acids (D-amino acids, in particular) have been reported to disrupt biofilm activity by integrating themselves into the bacterial cell wall, a hyperthermia-responsive gel was produced. The glycol chitin-based hydrogel was loaded with D-tyrosine, D-tryptophan and *D*-phenylalanine and reversed from a liquid state (at 4 °C) to a gel (at physiological temperature). Moreover, iron oxide NPs were incorporated in the gel, causing a magnetically induced hyperthermia that enhanced the cumulative release of the loaded amino acids. As a result, biofilms exposed to a 2 h gel treatment coupled with 10 min application of a magnetic field resulted in full biofilm disruption. In addition to CV staining, the authors also used cryo-SEM imaging for the biofilm assessments. It was demonstrated that following biofilm eradication with the formulation, no new colonies from the destroyed biofilms could be formed, strengthening the potential of the formulation to be used for the treatment of chronic infections, such as external wounds. However, biofilm-related infections in the human body can also
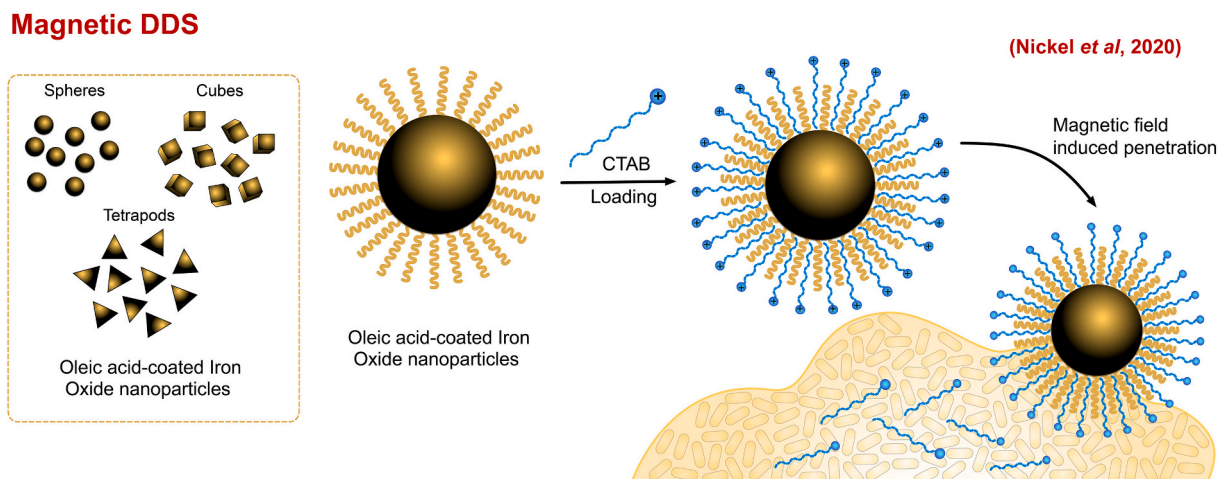
Magnetic DDS

Fig. 5. Development of nanomaterials with magnetic properties. Adapted from [153].

occur in the oral cavity and be caused by both bacteria and fungi. For such infections, root canal disinfectants are among the most commonly used treatments, however new systems are warranted to counteract the challenges caused by their inherent physicochemical properties. A new approach was therefore published by Ji *et al* [154] where the enzyme glucose oxidase (GOx) coated magnetic nanoparticles (Fe$_3$O$_4$) were prepared. For its synthesis, the team coupled aldehyde groups (in the glutaraldehyde cross-linker present in the nanoparticles) with amino groups in the enzyme. Using confocal microscopy and CV staining, the antibiofilm activity of the system was assessed in both bacteria and fungi, where the biofilm penetration of the particles increased if exposed to a magnetic field followed by biofilm destruction. >25 μm reduction in the average thickness of *Enterococcus faecalis* and *Candida albicans* biofilms was observed. This was related to the conversion of β-D glucose into H$_2$O$_2$, later catalyzed to •OH by the magnetic particles and/or bacterial oxidases and nutrient depletion induced by the enzyme.

Similar to temperature-triggered formulations, the published work regarding magnetic field as trigger for antibiofilm purposes is currently scarce, however the ideas developed thus far point to a promising strategy in the field of novel antibiofilm strategies.

6. Multiple stimuli-responsive

Many of the reported approaches that rely on internal triggers seek to achieve on-demand drug release and in some cases, a similar strategy has been demonstrated in carriers that rely on external triggers. Although internal and external triggers have pros and cons, their combination can potentially address rising challenges and contribute to enhanced antibacterial action. In this context, a variety of carriers can be designed to respond to more than one internal/external cue or combining one of each. As an example, carriers that respond to intrinsic biofilm features exert their action without requiring external stimuli. For instance, cutaneous biofilm can be treated with a dual internally responsive system (pH and enzyme) [155] or by internal/external responsive (pH and light) [156], whereas oral biofilms were destroyed by pH/redox-responsive nanoparticles [157]. Because many bacterial biofilms have variations in the matrix composition [158], the performance of the nanocarrier can differ. To avert this challenge, the combination of two internal cues for on-demand action can overcome differences in biofilm composition and achieve high antibiofilm activity. For example, in a pH/enzyme dual responsive system, even if certain biofilms have a lower-than-expected expression of the enzyme, the acidic pH might be enough to enhance potency of therapeutic agents. On the other hand, external triggers can be consciously applied for a

Table 4
Multiple stimuli responsive systems.

Active compound	Stimuli	Functions	System	Purpose	Reference
Vancomycin	pH and enzyme	pH-responsive lipids and lipase-degradable ester bonds in the lipid chain	DNA nanoparticles	Low pH protonates the ionizable lipid (otherwise neutral at physiological conditions) and lipases degrade the carrier for vancomycin-DNA NPs release	[155]
Chlorhexidine and silver ions	pH and redox	Disulfide bond-bridged organosilica moieties	Mesoporous nanoparticles	Disulfide bond-bridged organosilica moieties responded to pH and glutathione levels (glutathione induced the cleavage of the bonds)	[157]
Pifithrin-μ	pH and light	Zeolite-based imidazole framework (ZIF-8)	Mesoporous polydopamine nanoparticles	ZIF-8 degrades in acidic conditions and releases pifithrin-μ and zinc ions; The irradiation of the carrier generated heat due to the photothermal efficiency of the mesoporous polydopamine nanoparticles	[159]
Amoxicillin	pH and light	Zeolite-based imidazole framework (ZIF-8)	Pd-Cu nanoalloy	ZIF-8 degrades in acidic conditions and releases the antibiotic; The irradiation of the carrier generated heat due to the photothermal efficiency of Pd—Cu	[156]
Tannic acid, silver nanoparticles and gentamicin	pH, enzyme and magnetic nanoparticles (Fe$_3$O$_4$)	Hyaluronic acid and tannic acid	Multilayer film	Hyaluronic acid was used as outer shell for hyaluronidase-responsive action, and the silver nanoparticles dissolved in acidic conditions; The magnetic field enhanced biofilm penetration	[163]
Ascorbic acid (AA)	Enzyme and light	PTT and hyaluronic acid	Mesoporous ruthenium nanoparticles loaded with AA, coated with HA and an outer layer of ciprofloxacin-coated molybdenium dissulfide (MoS$_2$)	Combination of PTT with chemotherapy: HA coating had an enzyme-responsive function for Ascorbic acid (AA) release. Upon AA release, MoS$_2$ catalyzed the conversion to •OH. Laser application added the PTT effect due to photothermal properties of ruthenium NPs.	[73]
Ascorbic acid (AA)	Enzyme and light	PTT and hyaluronic acid	Graphene-mesoporous silica nanosheet loaded with AA, capped with HA-dopamine conjugates and an outer layer of vancomycin-coated ferromagnetic nanoparticles	Chemo-photothermal therapy due to photothermal properties of graphene. Hyaluronidase degraded the HA-dopamine, releasing AA, further catalyzed to •OH by ferromagnetic nanoparticles	[160]
Fluconazole and diketopyrrolopyrrole	Enzyme and light	PDT, PTT and lipase	poly(ethylene glycol)–poly(e-caprolactone) (PGL), fluconazole and diketopyrrolopyrrole	Enzyme-triggered degradation of the polymer for fluconazole release. The system also used photothermal and photodynamic properties of diketopyrrolopyrrole for combination treatment of these strategies with antibiotic action	[161]
Chlorin e6 and peptide	Enzyme and light	PDT and MMP-9	β-cyclodextrine with chlorin e6 core and outer shell of adamantane-terminated peptides	MMP cleaved the protective peptide of the nanoparticles, releasing chlorin e6 for photodynamic effect upon laser exposure	[162]

controlled response but might not be suitable for all biofilm sites. Therefore, the choice of system must be carefully envisioned according to the final application. Examples of multiple-stimuli responsive systems can be found in Table 4.

A dual internally responsive zwitterionic delivery system was recently developed in our group [155] against cutaneous biofilms with pH and enzyme-responsive characteristics. The carriers were composed of neutral (soy phosphatidylcholine), cationic ionizable (1,2-dioleyloxy-3-dimethylaminopropane) and anionic ((1,2-dipalmitoyl-sn-glycero-3-phospho((ethyl-1′,2′,3′-triazole) triethylene glycolmannose or cholesteryl hemisuccinate) lipids, which encapsulated DNA nanostructures for vancomycin delivery. A variety of nanoparticles were synthesized by varying molar ratio of the lipids, followed by the assessment of their impact on the physicochemical properties of the carriers. The optimized formulation resulted in a system that responded to the acidic pH of the infection environment by becoming positively charged (otherwise neutral at physiological pH) thus favoring biofilm accumulation and binding to the bacteria cell. Additionally, the carrier was degraded in the presence of lipase, which led to the release of vancomycin and the encapsulated DNA nanoparticles. Released DNA nanoparticles could interact with α-hemolysin (an important bacterial toxin) and mediate toxicity. Using CV staining and fluorescence intensity measurements, the carriers showed antibiofilm efficacy *in vitro* and in a porcine biofilm model, *in vivo* potency was confirmed. At higher concentrations of the formulation, an 87% reduction in the bacteria biomass was observed whilst a 99.68% reduction in the metabolic activity of fluorescently labelled *S. aureus* was reported. A different strategy was published by Lu and coworkers [157] with the release of chlorhexidine and silver ions from the dual redox and pH sensitive mesoporous nanoparticles against oral biofilms. The authors concluded that in presence of low pH and glutathione, the cumulative release of chlorhexidine and silver increased. Using MTS assays, the formulation inhibited biofilm growth with >60% reduction in biofilm viability after 72 h. Furthermore, confocal microscopy revealed that the formulation led to the weakest green signal and strongest red signal for *S. mutans* biofilms that were stained with the LIVE/DEAD bacterial viability kit. Whereas the first article was effective for wound therapy, this system was envisioned against oral biofilms, showing the versatility that dual-stimuli systems can bring.

Because the reduced potency of antibiotics can be further exacerbated during biofilm formation, reliance solely on internal triggers may fail to achieve clinical effect in humans. Therefore, efforts to drive synergism in antibacterial effect can be pursued *via* the design of smart carriers that show combined responsiveness to both external triggers (*e.g.*, light) and internal triggers (*e.g.*, pH or enzymes). Such combinations reveal novel opportunities for the development of complex carriers that generate greater responsiveness and can address biofilms formed by antimicrobial resistant strains (*e.g.*, MRSA). In two recent studies, light was used for photothermal therapy and combined with a pH responsive system. In a study by Peng *et al* [159], a carrier with a mesoporous polydopamine core (responsible for heat generation) and a zeolite-based imidazole framework (synthesized from zinc ions and 2-methylimidazole) as pH-responsive shell was developed. To strengthen the antibacterial activity of the particles, the carrier was loaded with Pifithrin-μ, an inhibitor of heat-shock protein, as means of lowering the tolerance of bacteria to heat. The shell degraded upon contact with acidic pH, releasing zinc ions (known to have antibacterial action), and Pifithrin-μ. Accordingly, *in vitro* and *in vivo* results demonstrated good potential for infected wound application due to effective anti-biofilm action combined with low damage for normal tissues. Similarly, Wang *et al* used zeolitic imidazolate framework-8 for its pH-responsive function but used Pd—Cu nanoalloy due to its photothermal properties [156]. The carrier was also loaded with amoxicillin and the acidic environment degraded the ZIF-8, leading to the release of an antibiotic that destroyed the bacterial wall. This made the bacteria more prone to the heat destruction after NIR irradiation. Using CV staining, the formulation caused 75.3%

and 74.8% inhibition of *S. aureus* and *P. aeruginosa* biofilms. In the absence of the antibiotic, only 49.4% and 42.4% inhibition of *S. aureus* and *P. aeruginosa* biofilms was observed under the same condition of NIR.

In another study, Liu and colleagues [73] first loaded the prodrug ascorbic acid into mesoporous ruthenium nanoparticles and coated the carrier with hyaluronic acid. Thereafter, ciprofloxacin-coated molybdenum disulfide (MoS$_2$) was subsequently bound to the surface. Ascorbic acid has pro-oxidant activities that promote the generation of H$_2$O$_2$, and can be converted into •OH radical under the action of peroxidases. Since MoS$_2$ has peroxidase-like activity, it was employed as a catalyst for the generation of •OH from ascorbic acid, and the antibiotic coating had a targeting function for both Gram-positive and Gram-negative bacteria. In the presence of bacteria-secreted hyaluronidase, the caping agent of the carrier was degraded. Moreover, the inclusion of ruthenium nanoparticles was as a result of its high NIR photothermal effect. Overall, a synergistic effect was achieved wherein degradation of hyaluronic acid enabled the release of ascorbic acid which was quickly catalyzed into •OH. Upon NIR laser irradiation, a photothermal induced bacterial destruction (91% removal of biofilms) was observed *via* crystal violet staining. The nanosystem was capable of biofilm destruction and inhibition of biofilms on implants. Additionally, wound healing properties in *in vivo* studies were observed in mice infection models. Replicating a similar concept for the generation of •OH, the group of Ji *et al* [160] developed in a nanoparticle loaded nanosheet carrier system wherein ascorbic acid was loaded together with ferromagnetic nanoparticles (for peroxidase activity). The system consisted of hyaluronic acid-capped graphene-mesoporous silica nanosheets loaded with ascorbic acid, to which vancomycin-coated magnetic nanoparticles were anchored. The exposure to hyaluronidase induced the degradation of the hyaluronic-dopamine conjugates that encapsulated the sheets, thus providing on-demand release of ascorbic acid, quickly converted to hydroxyl radical afterwards. Furthermore, due to the near-infrared absorption properties of graphene, the system showed chemo-photothermal and synergistic antibacterial effect. This was confirmed *in vivo* wherein catheters were co-incubated with *S. aureus* to induce biofilm formation and implanted in mice. The treatment resulted in gradual healing, providing evidence for the targeted and smart action for biofilm and bacterial destruction.

A study conducted by Yang and colleagues focused on the treatment of fungal biofilms using a lipase-responsive platform that combined photodynamic, photothermal and pharmacological action. The lipase-sensitive polymer poly(ethylene glycol)-poly(ε-caprolactone) was employed due to its stimuli-responsiveness and drug delivery action. The polymer was then combined with diketopyrrolopyrrole (used as photosensitizer for photothermal and photodynamic purposes) and fluconazole for synergistic effect. The degradation of poly(ε-caprolactone) in the presence of lipase released the drug and the combination of heat and ROS generation upon laser application resulted in anti-biofilm effect. Using CV staining, the authors showed that the combination of fluoconazole and diketopyrrolopyrrole in the formulation resulted in 72% destruction of biofilms. In the absence of the photosensitizer or drug, only 2% and 16% biofilm reduction were observed respectively. *In vivo* quantification of *C. albicans* colonies in infected wounds revealed only 3.4% survival of fungal cells after treatment with the multi-modal and synergistic antifungal nanoagent [161].

Han and colleagues explored the treatment of bacterial keratitis with a matrix-metaloproteinase-9-responsive nanoparticle allied with photodynamic effect. An enzyme-sensitive peptide (YGRKKKKRRQRRR-GPLGVRG-EEEEEE) terminated with adamantane was used as hydrophilic shell for the particle: its anionic nature prevented adhesion to healthy corneal cells, yet the EEEEEE peptide armor was cleaved at infections sites by MMP-9, exposing the positively charged peptide and enhancing its biofilm penetration. The hydrophobic core of the particle was composed of chlorin e6-conjugated β-cyclodextrin for increased ROS generation upon irradiation. Standard plate counting assay after treatment of *P. aeruginosa* biofilms with nanoparticle and irradiation

revealed over 99% of bactericidal effect. Moreover, *in vivo* testing of infected cornea of mice showed transparent corneas 7 days after treatment, with almost no colonies from the treated group. The team demonstrated that the exposure to the enzyme could change negatively charged particles into cationic carriers, enhancing their penetration into bacterial biofilms and further destroying bacteria upon irradiation [162].

In another work by Wang *et al* [163], a magnetic nanoplatform for enzyme and pH-triggered antimicrobial action was envisioned. For synthesis, the researchers used tannic acid, silver nanoparticles and gentamicin that were coated with magnetic nanoparticles. Using magnetic field navigation, the particles showed improved penetration into biofilms, and the use of hyaluronic acid as capping agent prevented premature drug release and acted together with tannic acid for pH-responsive action. The cumulative release of both gentamicin and Ag^+ ions were greater at a pH of 5.5 (compared to pH of 7.4) and in the presence of hyaluronidase. The antibacterial effect was enhanced by the use of an external magnetic field which allowed the nanoplatform to reach deeper layers in the biofilm, providing another promising strategy for biofilm tackling. Using SEM imaging and confocal microscopy, the authors observed destruction of the biofilm with low bacterial survival when treatment with the formulation was combined with an applied magnetic field. Additionally, bacteria colony counts demonstrated that in the absence of the magnetic field, 71–94% of bacteria survived within the biofilm whilst only 0.01–5% survival was seen when magnetic field was applied. These studies illustrate how different combinations can be used for on-demand drug release and the versatility they can bring as alternatives to plain antibiotic treatment.

7. Drug release from the different systems

The comparison between different stimuli on drug release profiles can be of major help for the design of smart delivery systems for biofilm therapy. Having shown increased antimicrobial action or decrease toxicity,stimuli-responsive delivery systems hold major importance for the clinic to reduce side effects for the patient without compromising the treatment efficacy. As seen in the previous section, different cues can be used to unleash antibacterial action, and the application of certain stimuli can influence the release behavior of a system by preventing undesired leakage of antimicrobials. Other reviews have discussed in detail drug release mechanisms for antibiofilm purposes, and the reader is directed to those for more in-depth information [164]. This section seeks to analyze how different stimuli-responsive approaches affect drug release profile and how it correlates with antibiofilm efficacy.

When administering a formulation in the clinic, the choice of stimulus should be carefully considered both for practical reasons and for drug release consequences. Whereas external triggers may offer the advantage of achieving a predictable release independently from biofilm features, (for example by turning the stimuli on and off), they are challenged by the fact that they still require a conscious application by the patient or caregiver and the presence of the stimuli itself. On the other hand, such complications are overcome if we look at internally responsive systems in which the biofilm milieu ensures drug release. However, given the physiological variability that characterizes biofilms (for example variations in pH values and enzyme concentrations), the release profile may vary from biofilm to biofilm, hence the response is not always predictable. It is noteworthy that different studies assessed drug release over different time periods (ranging from a few minutes to hours or days), and antibiofilm action was frequently assessed differently between studies, creating an additional challenge to effectively compare the different approaches. Nevertheless, it provides critical information on how drug release is affected by different formulations when similar or different stimuli are applied.

7.1. Externally-responsive systems

In light-responsive systems, drug release can be applied to achieve photothermal or photodynamic therapy both separately and simultaneously. In the first instance, the rule of thumb is the dependency of laser presence, often correlated with the applied power. Researchers have frequently observed that higher laser intensities generate overall higher temperatures, and the same temperature is reached faster. Since this cue is typically employed to destroy the chemical bond between drug and carrier, some studies show a faster release when using higher laser intensities. For example, the Pd nanocube loaded with hydrogen [116] developed by Yu and colleagues showed that the increase in laser intensity resulted in higher temperatures and faster hydrogen release. Turning the laser 'on' and 'off' showed a pronounced effect on the release, with no hydrogen leakage in the absence of stimuli. Such feature can be highly appreciated in the clinic as means of achieving a precisely controlled release system. It is worth noting that nearly all hydrogen was released after 30 min and this "on-and-off" laser approach, showed rapid release. Evaluation of the changes in OD_{550} values for biofilm biomass revealed that the sole photothermal effect diminished the value by 40% ($OD_{550} = 0.6$ for Pd + NIR treatment *versus* $OD_{550} = 1.0$ of NIR alone) and the combination of phototherapy and drug release achieved at least 90% reduction in *E. coli* and *S. aureus* (OD = 0.1 or less for treatment of PdH 50 μg/mL + NIR). A similar release profile was observed by Hua *et al* even though a different external stimulus was employed. The study assessed ciprofloxacin release from PLGA magnetic nano and microparticles under magnetic field. Both formulations had a 5% release in the absence of oscillating magnetic field over 6 h, yet a clear increase was observed when the magnetic field was applied, resulting in a $2\times$ increase in drug release. This application increased the inhibition rate of *P. aeruginosa* biofilms by a 10% and 5% (for micro and nanoparticles, respectively) compared to the same formulations in the absence of a magnetic field. In its presence, both achieved slightly over 30% of inhibition rate, assessed through XTT assay. Whilst the stimulus is different between these two studies, both showed how the application of an external stimuli can control and increase drug release for enhanced antibiofilm effect.

Other studies assessed NO release upon light trigger. The core material between the two systems was different (graphene platform [128] and metal transitional dichalcogenide sheet [104]), yet both observed a 20–30% NO release in 20–25 min in the absence of laser, which was increased to 90% after just 5 min of irradiation. After 10 min of irradiation, 80% of the biofilm was eliminated (assessed by biofilm staining with crystal violet) in the graphene study. Another study assessed the release profile of tobramycin at different temperatures and in three different liposomal formulations [130] where the ratio of distearoyl phosphatidylcholine, cypate and betainylated cholesterol were tailored. All three showed low release at physiological temperature (20% over 70 h) *versus* roughly 80% release over the same period at 45 °C, yet the release was different in the first 5 h, 60% release in the formulation with the highest cholesterol amounts *versus* 30% and 20% in the other two formulations. The liposomes with higher cholesterol content were able to eliminate 50–60% of biofilm after laser irradiation for 5 mins.

Photodynamic therapy can also be used for drug release purposes. A study evaluating thymol release [146] from chitosan micelles showed that under irradiation, the ROS generation led to thymol release. Light irradiation for 5 min led to 70% drug release over 30 h, 3-fold higher than in the absence of irradiation. Using crystal violet assay, the team reported that the formulation eliminated roughly 40% of L. *monocytogenes* and *S. aureus* biofilms without light irradiation as opposed to 80% or 70% (respectively) in its presence (relative biofilm value of 1.0 for control, and 0.6 or 0.2 without and with radiation for the loaded carrier in L. *monocytogenes* and 0.6 or 0.3 for *S. aureus* in the same conditions).

7.2. Internally-responsive systems

The presence of enzymes also has an impact on the drug release profile, often dependent on enzyme concentration. In the absence of enzymes, some systems exhibit no leakage whilst minimum release is observed for others. For example, some studies compared gelatinase [90] and hyaluronidase [82] responsiveness and showed some drug release over 48 h in the absence of enzyme, whereas a lipase study showed no release [165]. Furthermore, the lipase-responsive study showed pronounced bacterial killing efficacy in streptococcal biofilms in *S. mitis* and *S. mutans,* but not *S. salivarius* (evaluated by the percentage bacterial viability in biofilms). Such difference was attributed to high MIC values this strain has for the drug assessed (triclosan), yet it would be interesting to confirm if there are different enzyme concentrations between these strains that might impact drug release. Moreover, factors such as the composition and maturity of biofilms can have pronounced effects on enzyme expression, which would translate into different release profiles from the same system. It is noteworthy that the number of studies conducted are still lacking to provide comprehensive assessment on how different enzyme expression affects drug release and its correlation with biofilm destruction or inhibition, but this area is worth exploring.

pH-controlled drug release was assessed in different studies under acidic conditions, yet the assessed pH values differs between studies, ranging from 4.0 to 6.0. In the study conducted by Fullriede *et al* [74], the decrease in one pH unit (pH 4.0) was enough to increase the cumulative release of chlorhexidine from 240 μg/mg (pH 5.0) to 270 μg/mg in the first 12 h. Interestingly, the modification of the nanoporous silica particles to have pH responsiveness led to a lower cumulative release at physiological pH (7.4) and the release of the modified carriers under acidic conditions was still lower than the unmodified at neutral pH. After modification, the release was still superior in acidic conditions in a pH-dependent manner. Another study [81] showed faster release at pH 6 in comparison to pH 7.4, and the encapsulation of the drug into the responsive system led to controlled release with 69% of biofilm destruction comparatively to 26% of bare vancomycin, assessed through crystal violet assay.

7.3. Multiple stimuli-responsive systems

Considering systems that respond to more than one stimulus, internally responsive approaches were tested in two separate studies for dual pH and lipase responsiveness. The acidic pH triggered the protonation of the carrier to enhance biofilm penetration, whereas lipase triggered the release of the encapsulated drug. A study used zwitterionic lipid nanoparticles loaded with vancomycin containing DNA nanoparticles [155]. In this work, low lipase concentration led to 50% release in 24 h, which increased to 90% at higher enzyme concentrations. Interestingly, the study also observed that the system had a slower release in comparison to free vancomycin, but the amount released at 24 h was the same when using higher enzyme concentrations. Crystal violet staining method showed that biofilm biomass was reduced in 87% when treated with high concentrations of the formulation. A similar rationale was behind the work of Liu *et al*, where the presence of lipase enhanced the release of triclosan to 80–90% with a burst release from polymeric micelles in 50 h, and a reduction in metabolic activity in biofilms was observed for the carriers [79].

Attempts to control drug release using internal and external triggers simultaneously have been used such as combining pH and light. As an example, amoxicillin release was assessed after encapsulation in a zeolitic imidazolate framework-8 that encapsulated both the antibiotic and Pd—Cu nanoalloy [156]. This system had almost no release at pH 7.4, little over 10% for pH 6.0 and 60 to 80% release between the pH values of 5.0 and 3.0, respectively, in the absence of irradiation. To confirm the dual release hypothesis, the team evaluated release in the presence of both stimuli. At acidic pH of 5.5, release reached 30% over

50 min and increased to 40% upon laser irradiation for 10 min. At physiological pH (7.4) barely any drug was released irrespective of laser presence. Crystal violet staining results showed this approach resulted in 75% biofilm inhibition for *S. aureus* and *P. aeruginosa*.

8. Safety and toxicity considerations

The concept of toxicity as applied to nanoformulations is one of the major concerns when developing a formulation. The safety of the formulation is often dependent on the nanoparticle's properties, administration route and their interaction with surrounding environment. Their fate upon entering an organism can lead to acute or chronic toxic effects, unleash inflammatory responses, genotoxicity [166] and even embryo-fetal toxicity [167]. Since toxicity is not the main focus of this review, some general considerations are depicted, yet more in depth articles have been published elsewhere [168,169].

Many of the studies stated above focused on the development of smart drug delivery systems against biofilms for future applications in the clinic. While most assessed the toxicity of the systems through cell cytotoxicity assays or *in vivo* mouse model assays with satisfactory results, the use of nanotechnology still has some knowledge gaps when it comes to general and long-term safety. Most of the nanoparticles' features that affect toxicity are related to size, shape and surface chemistry since they influence the carrier's behavior inside cells and within the organism [170], causing the particles to manifest potential toxicity at tissue, cellular or molecular level. For example, size impacts the clearance and accumulation of the nanocarrier. In this context, intravenously administered, nanoparticles can be quickly cleared mainly through the kidneys (typically for sizes smaller than 6 nm) and liver (for sizes larger than 6 nm), or through the mononuclear phagocyte system where a long-term retention is observed [171]. However, long-term toxic effects can correlate with the accumulation of nanoparticles in certain organs such as the liver or spleen [172].

Surface chemistry also plays an important role regarding toxicity since the contact of nanoparticles with body fluids frequently alters their physicochemical properties. These changes can lead to aggregation or agglomeration and protein absorption on the corona; phenomena that interact closely with immune system. Whilst aggregation can lead to the formation of large particles, easily taken up by phagocytes, the surface coating of the particles could lead to enhanced or decreased immune recognition (through opsonization or dysopsonic effect [173]) or changes in the folding of plasma proteins, thus unleashing inflammatory reactions [174].

On a cellular level, nanoparticles can also lead to the generation of ROS which damages DNA, proteins, and lipids, and induce programmed cell death, which depends on the nanoparticle's size, dose, incubation period and charge [172]. In the context of ROS generation, the nanoparticle's composition can be of relevance. Metallic nanoparticles, such as silver, zinc or titanium can lead to ROS generation, mostly related to the release of metal ions [169], resulting from a catalytic process or a reduction with long term toxicity concerns [168]. Since metallic nanoparticles have been used in the synthesis of responsive nanoparticles for antibacterial purposes (*e.g.*, photothermal therapy), safety concerns should be considered in the development process. Other toxicity concerns named above are related to surface chemistry, size, and agglomeration are more dependent on the formulation and should be carefully chosen according to *in vivo* and *in vitro* studies based on acute and chronic exposure.

Administration route of the nanoparticles can play an additional role in the toxic effects, where the administration through the respiratory tract is more correlated with lung diseases, for example [175]. In this regard, most publications focus on parenteral, pulmonary and skin administration [176], yet biofilms can also be formed on ocular, oral or vaginal surfaces. Some nanoparticles are unable to reach deep parts of the eye, whilst smaller nanoparticles are gifted with this ability. The discrepancy opens the door to toxic responses not only to the anterior

segment of the eye (such as the cornea and conjunctiva) but also to sections on the posterior segment, such as the retina. Toxicity of the delivery system for this administration route has also shown a correlation with the material employed [177]. Another example concerns topical administration, where nanoparticle skin penetration is influenced according to the skin's integrity (damaged skin has a different influence on nanoparticle penetration in comparison to intact layers) and the size of the particle itself. It has been postulated that particles with 300 nm in size can reach deep skin layers without further penetration [178].

Apart from the system itself, the trigger can also cause body damage. For example, in photothermal therapy, tissue damage may occur due to inaccurate laser exposure or distribution of the photothermal agent [179]. Therefore, the development of smart nanoparticle-based formulations can bring tremendous potential for biomedical applications, yet extensive knowledge is necessary to prevent toxic side effects, where the choice of material, administration route and trigger must be carefully considered.

9. Conclusion and perspectives

Smart drug delivery systems represent an exciting alternative to current antimicrobial therapies given their potential to improve the penetration, potency and enhance the stability of antimicrobial therapies against biofilm related infections [164] caused by both susceptible and MDR strains. In this review, we highlighted how different smart drug delivery systems have been developed as antibiofilm strategies against bacterial and/or fungal biofilms paired with an analysis on their impact on drug release profiles. These systems offer on-demand controlled drug release by taking advantage of intrinsic biofilm characteristics or through the application of an external stimulus. Examples of the former include the characteristic acidic environment (where protonation can lead to the carrier destabilization) or the expression of certain enzymes (able to cleave chemical bonds to induce drug release). External stimuli typically focus on the application of a laser light or magnetic field for hyperthermia induction (thus breaking weak bonds between drug and carrier to release the loaded compound). Some researchers took a step further and used more than one stimulus for the treatment of cutaneous or oral biofilms [155,156]. Whilst there are plenty of triggers that can be used for on-demand drug delivery, biofilms can be formed on different surfaces of the human body and by different pathogens. Scientists should therefore consider that the same system might not be suitable for every location. For example, the use of a laser light might be suitable against skin infection but may not achieve the desired effect when applied against vaginal biofilms. Similarly, different pathogens tend to colonize different body surfaces, and therefore carriers that respond to internal cues might behave differently according to the species forming the biofilm.

Since the use of advanced systems against biofilms is quite at an embryonic state compared to the planktonic forms of bacteria [109], more integrated studies on the biological behavior of nanocarriers is still lacking under these conditions. This knowledge gap will hopefully be bridged through a more integrated assessment of toxicity and efficacy comparisons. Since there are plenty of cues that can be used for triggered drug release, direct comparisons between the different stimulus would be beneficial for the development of novel therapies. Furthermore, the development of a formulation should be tailored to the application site, which affects the toxicity profile it bears. Bearing this in mind, deeper knowledge on side effects is lacking. Furthermore, there is currently no universally accepted biofilm model that recapitulates fully the biological aspects of the different infection sites which therefore poses a significant translational challenge. Owing to the large complexity of *in vivo* biofilms, a unified effort is therefore needed within the research space.

Nonetheless, the novel strategies depicted in this review highlight the potential that smart drug delivery systems hold in the fight against biofilms. Hopefully, future developments in this field will contribute with innovative formulations for improved and safer antimicrobial alternatives.

CRediT authorship contribution statement

A. Sousa: Conceptualization, Writing – original draft, Writing – review & editing. **A. Ngoc Phung:** Writing – original draft. **N. Škalko-Basnet:** Writing – review & editing, Supervision, Funding acquisition. **S. Obuobi:** Project administration, Conceptualization, Writing – original draft, Writing – review & editing, Supervision, Funding acquisition.

Declaration of Competing Interest

None.

Data availability

No data was used for the research described in the article.

Acknowledgement

References

[1] S. Tan, Y. Tatsumura, Alexander Fleming (1881–1955): discoverer of penicillin, Singap. Med. J. 56 (07) (Jul. 2015) 366–367, https://doi.org/10.11622/smedj.2015105.

[2] B.L. Ligon, Penicillin: its discovery and early development, Semin. Pediatr. Infect. Dis. 15 (1) (Jan. 2004) 52–57, https://doi.org/10.1053/j.spid.2004.02.001.

[3] G. Gebreyohannes, A. Nyerere, C. Bii, D.B. Sbhatu, Challenges of intervention, treatment, and antibiotic resistance of biofilm-forming microorganisms, Heliyon 5 (8) (Aug. 2019), e02192, https://doi.org/10.1016/j.heliyon.2019.e02192.

[4] D. Sharma, L. Misba, A.U. Khan, Antibiotics versus biofilm: an emerging battleground in microbial communities, Antimicrob. Resist. Infect. Control 8 (Dec. 2019) 76, https://doi.org/10.1186/s13756-019-0533-3.

[5] N. Singh, et al., Dual bioresponsive antibiotic and quorum sensing inhibitor combination nanoparticles for treatment of: Pseudomonas aeruginosa biofilms in vitro and ex vivo, Biomater. Sci. 7 (10) (2019) 4099–4111, https://doi.org/10.1039/c9bm00773c.

[6] Y. Zhang, et al., Bacteria responsive polyoxometalates nanocluster strategy to regulate biofilm microenvironments for enhanced synergetic antibiofilm activity and wound healing, Theranostics 10 (22) (2020) 10031–10045, https://doi.org/10.7150/thno.49008.

[7] H. Koo, R.N. Allan, R.P. Howlin, P. Stoodley, L. Hall-Stoodley, Targeting microbial biofilms: current and prospective therapeutic strategies, Nat. Rev. Microbiol. 15 (12) (Dec. 2017) 740–755, https://doi.org/10.1038/nrmicro.2017.99.

[8] A. Brauner, O. Fridman, O. Gefen, N.Q. Balaban, Distinguishing between resistance, tolerance and persistence to antibiotic treatment, Nat. Rev. Microbiol. 14 (5) (2016) 320–330, https://doi.org/10.1038/nrmicro.2016.34.

[9] R.M. Donlan, J.W. Costerton, Biofilms: survival mechanisms of clinically relevant microorganisms, Clin. Microbiol. Rev. 15 (2) (Apr. 2002) 167–193, https://doi.org/10.1128/CMR.15.2.167-193.2002.

[10] J. Armitano, V. Méjean, C. Jourlin-Castelli, Gram-negative bacteria can also form pellicles, Environ. Microbiol. Rep. 6 (6) (2014) 534–544, https://doi.org/10.1111/1758-2229.12171.

[11] D. Banerjee, P.M. Shivapriya, P.K. Gautam, K. Misra, A.K. Sahoo, S.K. Samanta, A review on basic biology of bacterial biofilm infections and their treatments by nanotechnology-based approaches, Proc. Natl. Acad. Sci. India Sect. B Biol. Sci. 90 (2) (Jun. 2020) 243–259, https://doi.org/10.1007/s40011-018-01065-7.

[12] A.D. Verderosa, M. Totsika, K.E. Fairfull-Smith, Bacterial biofilm eradication agents: a current review, Front. Chem. 7 (November) (2019) 1–17, https://doi.org/10.3389/fchem.2019.00824.

[13] X. Zhu, A.F. Radovic-Moreno, J. Wu, R. Langer, J. Shi, Nanomedicine in the management of microbial infection – overview and perspectives, Nano Today 9 (4) (Aug. 2014) 478–498, https://doi.org/10.1016/j.nantod.2014.06.003.

[14] K. Sauer, et al., The biofilm life cycle: expanding the conceptual model of biofilm formation, Nat. Rev. Microbiol. 20 (10) (2022) 608–620, https://doi.org/10.1038/s41579-022-00767-0.

[15] R. Ferrer-Espada, H. Shahrour, B. Pitts, P.S. Stewart, S. Sánchez-Gómez, G. Martínez-de-Tejada, A permeability-increasing drug synergizes with bacterial efflux pump inhibitors and restores susceptibility to antibiotics in multi-drug resistant Pseudomonas aeruginosa strains, Sci. Rep. 9 (1) (2019) 1–12, https://doi.org/10.1038/s41598-019-39659-4.

[16] G. Feng, Y. Cheng, S.-Y. Wang, D.A. Borca-Tasciuc, R.W. Worobo, C.I. Moraru, Bacterial attachment and biofilm formation on surfaces are reduced by small-diameter nanoscale pores: how small is small enough? npj Biofilms Microb. 1 (1) (Dec. 2015) 15022, https://doi.org/10.1038/npjbiofilms.2015.22.

[17] L. Kirchhoff, et al., Biofilm formation of the black yeast-like fungus Exophiala dermatitidis and its susceptibility to antiinfective agents, Sci. Rep. 7 (1) (Mar. 2017) 42886, https://doi.org/10.1038/srep42886.

[18] L. Neu, C.R. Proctor, J.-C. Walser, F. Hammes, Small-scale heterogeneity in drinking water biofilms, Front. Microbiol. 10 (Oct. 2019), https://doi.org/10.3389/fmicb.2019.02446.

[19] V. Leung, C.M. Lévesque, A stress-inducible quorum-sensing peptide mediates the formation of Persister cells with noninherited multidrug tolerance, J. Bacteriol. 194 (9) (May 2012) 2265–2274, https://doi.org/10.1128/JB.06707-11.

[20] J. Soler-Arango, C. Figoli, G. Muraca, A. Bosch, G. Brelles-Mariño, The Pseudomonas aeruginosa biofilm matrix and cells are drastically impacted by gas discharge plasma treatment: a comprehensive model explaining plasma-mediated biofilm eradication, PLoS One 14 (6) (Jun. 2019), e0216817, https://doi.org/10.1371/journal.pone.0216817.

[21] E.J. Stewart, M. Ganesan, J.G. Younger, M.J. Solomon, Artificial biofilms establish the role of matrix interactions in staphylococcal biofilm assembly and disassembly, Sci. Rep. 5 (1) (Oct. 2015) 13081, https://doi.org/10.1038/srep13081.

[22] E.K. Davenport, D.R. Call, H. Beyenal, Differential protection from tobramycin by extracellular polymeric substances from Acinetobacter baumannii and Staphylococcus aureus biofilms, Antimicrob. Agents Chemother. 58 (8) (Aug. 2014) 4755–4761, https://doi.org/10.1128/AAC.03071-14.

[23] N. Billings, et al., The extracellular matrix component Psl provides fast-acting antibiotic defense in Pseudomonas aeruginosa biofilms, PLoS Pathog. 9 (8) (Aug. 2013), e1003526, https://doi.org/10.1371/journal.ppat.1003526.

[24] J.V. Desai, A.P. Mitchell, D.R. Andes, Fungal biofilms, drug resistance, and recurrent infection, Cold Spring Harb. Perspect. Med. 4 (10) (Oct. 2014) a019729, https://doi.org/10.1101/cshperspect.a019729.

[25] T.-O. Peulen, K.J. Wilkinson, Diffusion of nanoparticles in a biofilm, Environ. Sci. Technol. 45 (8) (Apr. 2011) 3367–3373, https://doi.org/10.1021/es103450g.

[26] J. Kreth, et al., Quantitative analyses of Streptococcus mutans biofilms with quartz crystal microbalance, microjet impingement and confocal microscopy, Biofilms 1 (4) (Oct. 2004) 277–284, https://doi.org/10.1017/S1479050504001516.

[27] K. Quan, et al., Artificial channels in an infectious biofilm created by magnetic nanoparticles enhanced bacterial killing by antibiotics, Small 15 (39) (2019) 1–6, https://doi.org/10.1002/smll.201902313.

[28] R.M. Pinto, F.A. Soares, S. Reis, C. Nunes, P. Van Dijck, Innovative strategies toward the disassembly of the EPS matrix in bacterial biofilms, Front. Microbiol. 11 (May) (2020) 1–20, https://doi.org/10.3389/fmicb.2020.00952.

[29] W. Li, et al., Insights into the role of extracellular DNA and extracellular proteins in biofilm formation of Vibrio parahaemolyticus, Front. Microbiol. 11 (May 2020), https://doi.org/10.3389/fmicb.2020.00813.

[30] R. Fanaei Pirlar, M. Emaneini, R. Beigverdi, M. Banar, W.B. van Leeuwen, F. Jabalameli, Combinatorial effects of antibiotics and enzymes against dual-species Staphylococcus aureus and Pseudomonas aeruginosa biofilms in the wound-like medium, PLoS One 15 (6) (Jun. 2020), e0235093, https://doi.org/10.1371/journal.pone.0235093.

[31] L. Zhou, Y. Zhang, Y. Ge, X. Zhu, J. Pan, Regulatory mechanisms and promising applications of quorum sensing-inhibiting agents in control of bacterial biofilm formation, Front. Microbiol. 11 (Oct. 2020), https://doi.org/10.3389/fmicb.2020.589640.

[32] S.T. Rutherford, B.L. Bassler, Bacterial quorum sensing: its role in virulence and possibilities for its control, Cold Spring Harb. Perspect. Med. 2 (11) (Nov. 2012) a012427, https://doi.org/10.1101/cshperspect.a012427.

[33] P. Saxena, Y. Joshi, K. Rawat, R. Bisht, Biofilms: architecture, resistance, quorum sensing and control mechanisms, Indian J. Microbiol. 59 (1) (Mar. 2019) 3–12, https://doi.org/10.1007/s12088-018-0757-6.

[34] K. Qvortrup, et al., Small molecule anti-biofilm agents developed on the basis of mechanistic understanding of biofilm formation, Front. Chem. 7 (Nov. 2019), https://doi.org/10.3389/fchem.2019.00742.

[35] B. LaSarre, M.J. Federle, Exploiting quorum sensing to confuse bacterial pathogens, Microbiol. Mol. Biol. Rev. 77 (1) (Mar. 2013) 73–111, https://doi.org/10.1128/MMBR.00046-12.

[36] E. Paluch, J. Rewak-Soroczyńska, I. Jędrusik, E. Mazurkiewicz, K. Jermakow, Prevention of biofilm formation by quorum quenching, Appl. Microbiol. Biotechnol. 104 (5) (Mar. 2020) 1871–1881, https://doi.org/10.1007/s00253-020-10349-w.

[37] W.-J. Cheng, et al., Quorum sensing inhibition and tobramycin acceleration in Chromobacterium violaceum by two natural cinnamic acid derivatives, Appl. Microbiol. Biotechnol. 104 (11) (Jun. 2020) 5025–5037, https://doi.org/10.1007/s00253-020-10593-w.

[38] G. Ramage, S.P. Saville, B.L. Wickes, J.L. López-Ribot, Inhibition of Candida albicans biofilm formation by Farnesol, a quorum-sensing molecule, Appl. Environ. Microbiol. 68 (11) (Nov. 2002) 5459–5463, https://doi.org/10.1128/AEM.68.11.5459-5463.2002.

[39] T.K. Wood, S.J. Knabel, B.W. Kwan, Bacterial Persister cell formation and dormancy, Appl. Environ. Microbiol. 79 (23) (Dec. 2013) 7116–7121, https://doi.org/10.1128/AEM.02636-13.

[40] T. Hossain, H.S. Deter, E.J. Peters, N.C. Butzin, Antibiotic tolerance, persistence, and resistance of the evolved minimal cell, mycoplasma mycoides JCVI-Syn3B, iScience 24 (5) (May 2021), 102391, https://doi.org/10.1016/j.isci.2021.102391.

[41] B.W. Kwan, N. Chowdhury, T.K. Wood, Combatting bacterial infections by killing persister cells with mitomycin C, Environ. Microbiol. 17 (11) (Nov. 2015) 4406–4414, https://doi.org/10.1111/1462-2920.12873.

[42] N. Chowdhury, T.L. Wood, M. Martínez-Vázquez, R. García-Contreras, T.K. Wood, DNA-crosslinker cisplatin eradicates bacterial persister cells, Biotechnol. Bioeng. 113 (9) (Sep. 2016) 1984–1992, https://doi.org/10.1002/bit.25963.

[43] X. Chen, M. Zhang, C. Zhou, N.R. Kallenbach, D. Ren, Control of bacterial persister cells by Trp/Arg-containing antimicrobial peptides, Appl. Environ. Microbiol. 77 (14) (Jul. 2011) 4878–4885, https://doi.org/10.1128/AEM.02440-10.

[44] K.R. Allison, M.P. Brynildsen, J.J. Collins, Metabolite-enabled eradication of bacterial persisters by aminoglycosides, Nature 473 (7346) (May 2011) 216–220, https://doi.org/10.1038/nature10069.

[45] N.-Y. Lee, W.-C. Ko, P.-R. Hsueh, Nanoparticles in the treatment of infections caused by multidrug-resistant organisms, Front. Pharmacol. 10 (Oct. 2019), https://doi.org/10.3389/fphar.2019.01153.

[46] J. Talapko, T. Matijević, M. Juzbašić, A. Antolović-Požgain, I. Škrlec, Antibacterial activity of Silver and its application in dentistry, cardiology and dermatology, Microorganisms 8 (9) (Sep. 2020) 1400, https://doi.org/10.3390/microorganisms8091400.

[47] J. Gopal, N. Hasan, M. Manikandan, H.-F. Wu, Bacterial toxicity/compatibility of platinum nanospheres, nanocuboids and nanoflowers, Sci. Rep. 3 (1) (Dec. 2013) 1260, https://doi.org/10.1038/srep01260.

[48] D.L. Slomberg, Y. Lu, A.D. Broadnax, R.A. Hunter, A.W. Carpenter, M.H. Schoenfisch, Role of size and shape on biofilm eradication for nitric oxide-releasing silica nanoparticles, ACS Appl. Mater. Interfaces 5 (19) (Oct. 2013) 9322–9329, https://doi.org/10.1021/am402618w.

[49] M. Khan, et al., Enhanced antimicrobial activity of biofunctionalized zirconia nanoparticles, ACS Omega 5 (4) (Feb. 2020) 1987–1996, https://doi.org/10.1021/acsomega.9b03840.

[50] Y. Liu, et al., The enhanced permeability and retention effect based nanomedicine at the site of injury, Nano Res. 13 (2) (Feb. 2020) 564–569, https://doi.org/10.1007/s12274-020-2655-6.

[51] E.G. Di Domenico, et al., Microbial biofilm correlates with an increased antibiotic tolerance and poor therapeutic outcome in infective endocarditis, BMC Microbiol. 19 (1) (Dec. 2019) 228, https://doi.org/10.1186/s12866-019-1596-2.

[52] A.R. Kirtane, M. Verma, P. Karandikar, J. Furin, R. Langer, G. Traverso, Nanotechnology approaches for global infectious diseases, Nat. Nanotechnol. 16 (4) (Apr. 2021) 369–384, https://doi.org/10.1038/s41565-021-00866-8.

[53] D. Liu, F. Yang, F. Xiong, N. Gu, The smart drug delivery system and its clinical potential, Theranostics 6 (9) (2016) 1306–1323, https://doi.org/10.7150/thno.14858.

[54] V.R. Cherkasov, E.N. Mochalova, A.V. Babenyshev, A.V. Vasilyeva, P.I. Nikitin, M.P. Nikitin, Nanoparticle beacons: supersensitive smart materials with on/off-switchable affinity to biomedical targets, ACS Nano 14 (2) (Feb. 2020) 1792–1803, https://doi.org/10.1021/acsnano.9b07569.

[55] G. Guan, M. Wu, M. Han, Stimuli-responsive hybridized nanostructures, Adv. Funct. Mater. 30 (2) (Jan. 2020) 1903439, https://doi.org/10.1002/adfm.201903439.

[56] A.H. Chen, P.A. Silver, Designing biological compartmentalization, Trends Cell Biol. 22 (12) (Dec. 2012) 662–670, https://doi.org/10.1016/j.tcb.2012.07.002.

[57] A. Sikder, A. Chaudhuri, S. Mondal, N.D.P. Singh, Recent advances on stimuli-responsive combination therapy against multidrug-resistant bacteria and biofilm, ACS Appl. Bio Mater. 4 (6) (2021) 4667–4683, https://doi.org/10.1021/acsabm.1c00150.

[58] Y. Huang, L. Zou, J. Wang, Q. Jin, J. Ji, Stimuli-responsive nanoplatforms for antibacterial applications, Wiley Interdiscip. Rev. Nanomed. Nanobiotechnol. (2022) 1–21, https://doi.org/10.1002/wnan.1775. December 2021.

[59] R. Canaparo, F. Foglietta, F. Giuntini, C. Della Pepa, F. Dosio, L. Serpe, Recent developments in antibacterial therapy: and therapeutic nanoparticles, Molecules. 24 (2019) 1–15.

[60] M. Ding, W. Zhao, L.J. Song, S.F. Luan, Stimuli-responsive nanocarriers for bacterial biofilm treatme, Rare Metals (2021), https://doi.org/10.1007/s12598-021-01802-4.

[61] G. Kocak, C. Tuncer, V. Bütün, pH-responsive polymers, Polym. Chem. 8 (1) (2017) 144–176, https://doi.org/10.1039/C6PY01872F.

[62] W. Zhang, L. Shi, R. Ma, Y. An, Y. Xu, K. Wu, Micellization of thermo- and pH-responsive triblock copolymer of poly(ethylene glycol)- b -poly(4-vinylpyridine)- b -poly (N -isopropylacrylamide), Macromolecules 38 (21) (Oct. 2005) 8850–8852, https://doi.org/10.1021/ma050998o.

[63] A.S.M. Wong, et al., Self-assembling dual component nanoparticles with endosomal escape capability, Soft Matter 11 (15) (2015) 2993–3002, https://doi.org/10.1039/C5SM00082C.

[64] O. Sedláček, et al., Polymer conjugates of acridine-type anticancer drugs with pH-controlled activation, Bioorg. Med. Chem. 20 (13) (Jul. 2012) 4056–4063, https://doi.org/10.1016/j.bmc.2012.05.007.

[65] G.F. Walker, et al., Toward synthetic viruses: endosomal pH-triggered deshielding of targeted polyplexes greatly enhances gene transfer in vitro and in vivo, Mol.

Ther. 11 (3) (Mar. 2005) 418–425, https://doi.org/10.1016/j.ymthe.2004.11.006.

[66] H. Li, et al., On-demand combinational delivery of curcumin and doxorubicin via a pH-labile micellar nanocarrier, Int. J. Pharm. 495 (1) (Nov. 2015) 572–578, https://doi.org/10.1016/j.ijpharm.2015.09.022.

[67] Y. Gu, Y. Zhong, F. Meng, R. Cheng, C. Deng, Z. Zhong, Acetal-linked paclitaxel prodrug micellar nanoparticles as a versatile and potent platform for cancer therapy, Biomacromolecules 14 (8) (Aug. 2013) 2772–2780, https://doi.org/10.1021/bm400615n.

[68] E.R. Gillies, A.P. Goodwin, J.M.J. Fréchet, Acetals as pH-sensitive linkages for drug delivery, Bioconjug. Chem. 15 (6) (Nov. 2004) 1254–1263, https://doi.org/10.1021/bc049853x.

[69] H. Feng, Y. Sun, J. Zhang, L. Deng, A. Dong, Influence of supramolecular layer-crosslinked structure on stability of dual pH-responsive polymer nanoparticles for doxorubicin delivery, J. Drug Deliv. Sci. Technol. 45 (Jun. 2018) 81–92, https://doi.org/10.1016/j.jddst.2018.03.008.

[70] H.S. Han, et al., Bioreducible shell-cross-linked hyaluronic acid nanoparticles for tumor-targeted drug delivery, Biomacromolecules 16 (2) (Feb. 2015) 447–456, https://doi.org/10.1021/bm5017755.

[71] K.H. Min, et al., pH-responsive mineralized nanoparticles for bacteria-triggered topical release of antibiotics, J. Ind. Eng. Chem. 71 (2019) 210–219, https://doi.org/10.1016/j.jiec.2018.11.027.

[72] P. Li, et al., Design of pH-responsive dissociable nanosystem based on carbon dots with enhanced anti-biofilm property and excellent biocompatibility, ACS Appl. Bio Mater. 3 (2) (2020) 1105–1115, https://doi.org/10.1021/acsabm.9b01053.

[73] Y. Liu, et al., Enzyme-responsive mesoporous ruthenium for combined chemo-photothermal therapy of drug-resistant bacteria, ACS Appl. Mater. Interfaces 11 (30) (2019) 26590–26606, https://doi.org/10.1021/acsami.9b07866.

[74] H. Fullriede, et al., PH-responsive release of chlorhexidine from modified nanoporous silica nanoparticles for dental applications, BioNanoMaterials 17 (1–2) (2016) 59–72, https://doi.org/10.1515/bnm-2016-0003.

[75] T. Niaz, S. Shabbir, T. Noor, R. Abbasi, M. Imran, Alginate-caseinate based pH-responsive nano-coacervates to combat resistant bacterial biofilms in oral cavity, Int. J. Biol. Macromol. 156 (2020) 1366–1380, https://doi.org/10.1016/j.ijbiomac.2019.11.177.

[76] D. Hassan, C.A. Omolo, V.O. Fasiku, C. Mocktar, T. Govender, Novel chitosan-based pH-responsive lipid-polymer hybrid nanovesicles (OLA-LPHVs) for delivery of vancomycin against methicillin-resistant Staphylococcus aureus infections, Int. J. Biol. Macromol. 147 (2020) 385–398, https://doi.org/10.1016/j.ijbiomac.2020.01.019.

[77] Z. Zhao, C. Ding, Y. Wang, H. Tan, J. Li, PH-responsive polymeric nanocarriers for efficient killing of cariogenic bacteria in biofilms, Biomater. Sci. 7 (4) (2019) 1643–1651, https://doi.org/10.1039/c8bm01640b.

[78] Z. Zhou, et al., PH-activated nanoparticles with targeting for the treatment of oral plaque biofilm, J. Mater. Chem. B 6 (4) (2018) 586–592, https://doi.org/10.1039/c7tb02682j.

[79] Y. Liu, et al., Surface-adaptive, antimicrobially loaded, micellar nanocarriers with enhanced penetration and killing efficiency in staphylococcal biofilms, ACS Nano 10 (4) (2016) 4779–4789, https://doi.org/10.1021/acsnano.6b01370.

[80] B. Horev, et al., PH-activated nanoparticles for controlled topical delivery of farnesol to disrupt oral biofilm virulence, ACS Nano 9 (3) (2015) 2390–2404, https://doi.org/10.1021/nn507170s.

[81] Y. Jaglal, N. Osman, C.A. Omolo, C. Mocktar, N. Devnarain, T. Govender, Formulation of pH-responsive lipid-polymer hybrid nanoparticles for co-delivery and enhancement of the antibacterial activity of vancomycin and 18β-glycyrrhetinic acid, J. Drug Deliv. Sci. Technol 64 (2021) 102607, https://doi.org/10.1016/j.jddst.2021.102607. December 2020.

[82] B. Wang, et al., Construction of high drug loading and enzymatic degradable multilayer films for self-defense drug release and long-term biofilm inhibition, Biomacromolecules 19 (1) (2018) 85–93, https://doi.org/10.1021/acs.biomac.7b01268.

[83] G. Cado, et al., Self-defensive biomaterial coating against bacteria and yeasts: polysaccharide multilayer film with embedded antimicrobial peptide, Adv. Funct. Mater. 23 (38) (2013) 4801–4809, https://doi.org/10.1002/adfm.201300416.

[84] Y. Liu, et al., Nanocarriers with conjugated antimicrobials to eradicate pathogenic biofilms evaluated in murine in vivo and human ex vivo infection models, Acta Biomater. 79 (2018) 331–343, https://doi.org/10.1016/j.actbio.2018.08.038.

[85] T. Wang, et al., Nanovalves-based Bacteria-triggered, self-defensive antibacterial coating: using combination therapy, dual stimuli-responsiveness, and multiple release modes for treatment of implant-associated infections, Chem. Mater. 29 (19) (Oct. 2017) 8325–8337, https://doi.org/10.1021/acs.chemmater.7b02678.

[86] Y. Su, L. Zhao, F. Meng, Z. Qiao, Y. Yao, J. Luo, Triclosan loaded polyurethane micelles with pH and lipase sensitive properties for antibacterial applications and treatment of biofilms, Mater. Sci. Eng. C 93 (Dec. 2018) 921–930, https://doi.org/10.1016/j.msec.2018.08.063.

[87] Y.N. Albayaty, et al., Enzyme responsive copolymer micelles enhance the anti-biofilm efficacy of the antiseptic chlorhexidine, Int. J. Pharm. 566 (2019) 329–341, https://doi.org/10.1016/j.ijpharm.2019.05.069.

[88] M.-H. Xiong, Y.-J. Li, Y. Bao, X.-Z. Yang, B. Hu, J. Wang, Bacteria-responsive multifunctional nanogel for targeted antibiotic delivery, Adv. Mater. 24 (46) (Dec. 2012) 6175–6180, https://doi.org/10.1002/adma.201202847.

[89] S. Thamphiwatana, et al., Phospholipase A2-responsive antibiotic delivery via nanoparticle-stabilized liposomes for the treatment of bacterial infection, J. Mater. Chem. B 2 (46) (Sep. 2014) 8201–8207, https://doi.org/10.1039/C4TB01110D.

[90] J. Xu, et al., Microneedle patch-mediated treatment of bacterial biofilms, ACS Appl. Mater. Interfaces 11 (16) (Apr. 2019) 14640–14646, https://doi.org/10.1021/acsami.9b02578.

[91] J.J. Li, et al., Lactose azocalixarene drug delivery system for the treatment of multidrug-resistant pseudomonas aeruginosa infected diabetic ulcer, Nat. Commun. 13 (1) (2022) 1–12, https://doi.org/10.1038/s41467-022-33920-7.

[92] V.V. Komnatnyy, W.C. Chiang, T. Tolker-Nielsen, M. Givskov, T.E. Nielsen, Bacteria-triggered release of antimicrobial agents, Angew. Chem. Int. Ed. 53 (2) (2014) 439–441, https://doi.org/10.1002/anie.201307975.

[93] C. Novotný, et al., Biodegradation of aromatic-aliphatic copolyesters and polyesteramides by esterase activity-producing microorganisms, Int. Biodeterior. Biodegrad. 97 (2015) 25–30, https://doi.org/10.1016/j.ibiod.2014.10.010.

[94] Z. Zhang, et al., Macrocyclic-amphiphile-based self-assembled nanoparticles for ratiometric delivery of therapeutic combinations to tumors, Adv. Mater. 33 (12) (2021), https://doi.org/10.1002/adma.202007719.

[95] S.H. Yun, S.J.J. Kwok, Light in diagnosis, therapy and surgery, Nat. Biomed. Eng. 1 (1) (Jan. 2017) 0008, https://doi.org/10.1038/s41551-016-0008.

[96] H.P. Lee, A.K. Gaharwar, Light-responsive inorganic biomaterials for biomedical applications, Adv. Sci. 7 (17) (2020), https://doi.org/10.1002/advs.202000863.

[97] D. Barolet, F. Christiaens, M.R. Hamblin, Infrared and skin: friend or foe, J. Photochem. Photobiol. B Biol. 155 (2016) 78–85, https://doi.org/10.1016/j.jphotobiol.2015.12.014.

[98] T. Cui, S. Wu, Y. Sun, J. Ren, X. Qu, Self-propelled active photothermal nanoswimmer for deep-layered elimination of biofilm in vivo, Nano Lett. 20 (10) (2020) 7350–7358, https://doi.org/10.1021/acs.nanolett.0c02767.

[99] Z. Huang, et al., Synthesis of carbon quantum dot-poly lactic-co-glycolic acid hybrid nanoparticles for chemo-photothermal therapy against bacterial biofilms, J. Colloid Interface Sci. 577 (2020) 66–74, https://doi.org/10.1016/j.jcis.2020.05.067.

[100] S. Yu, G. Li, R. Liu, D. Ma, W. Xue, Dendritic Fe3O4@poly(dopamine)@PAMAM nanocomposite as controllable NO-releasing material: a synergistic photothermal and NO antibacterial study, Adv. Funct. Mater. 28 (20) (2018) 1–14, https://doi.org/10.1002/adfm.201707440.

[101] J. Zhu, et al., L-Arg-rich amphiphilic dendritic peptide as a versatile NO donor for NO / photodynamic synergistic treatment of bacterial infections and promoting wound healing, Small 17 (32) (2021) 2101495, https://doi.org/10.1002/smll.202101495.

[102] W. Ma, et al., Ultra-efficient antibacterial system based on photodynamic therapy and CO gas therapy for synergistic antibacterial and ablation biofilms, ACS Appl. Mater. Interfaces 12 (20) (2020) 22479–22491, https://doi.org/10.1021/acsami.0c01967.

[103] Z. Yuan, et al., Near-infrared light-triggered nitric-oxide-enhanced photodynamic therapy and low-temperature photothermal therapy for biofilm elimination, ACS Nano 14 (3) (2020) 3546–3562, https://doi.org/10.1021/acsnano.9b09871.

[104] C. Zhang, et al., Polyphenol-assisted exfoliation of transition metal dichalcogenides into nanosheets as photothermal nanocarriers for enhanced antibiofilm activity, ACS Nano 12 (12) (2018) 12347–12356, https://doi.org/10.1021/acsnano.8b06321.

[105] W. Li, X. Geng, D. Liu, Z. Li, Near-infrared light-enhanced protease-conjugated gold nanorods as a photothermal antimicrobial agent for elimination of exotoxin and biofilms, Int. J. Nanomedicine 14 (2019) 8047–8058, https://doi.org/10.2147/IJN.S212750.

[106] J. Estelrich, M. Antònia Busquets, Iron oxide nanoparticles in photothermal therapy, Molecules 23 (7) (2018), https://doi.org/10.3390/molecules23071567.

[107] G. Dacarro, A. Taglietti, P. Pallavicini, Prussian blue nanoparticles as a versatile photothermal tool, Molecules 23 (6) (2018) 1–20, https://doi.org/10.3390/molecules23061414.

[108] D.J. de Aberasturi, A.B. Serrano-Montes, L.M. Liz-Marzán, Modern applications of plasmonic nanoparticles: from energy to health, Adv. Opt. Mater. 3 (5) (May 2015) 602–617, https://doi.org/10.1002/adom.201500053.

[109] G. Qing, et al., Thermo-responsive triple-function nanotransporter for efficient chemo-photothermal therapy of multidrug-resistant bacterial infection, Nat. Commun. 10 (1) (2019) 1–12, https://doi.org/10.1038/s41467-019-12313-3.

[110] W.L. Chiang, et al., A rapid drug release system with a NIR light-activated molecular switch for dual-modality photothermal/antibiotic treatments of subcutaneous abscesses, J. Control. Release 199 (2015) 53–62, https://doi.org/10.1016/j.jconrel.2014.12.011.

[111] L. Zhang, et al., Photon-responsive antibacterial nanoplatform for synergistic photothermal-/pharmaco-therapy of skin infection, ACS Appl. Mater. Interfaces 11 (1) (2019) 300–310, https://doi.org/10.1021/acsami.8b18146.

[112] S.J. Norton, T. Vo-Dinh, Photothermal effects of plasmonic metal nanoparticles in a fluid, J. Appl. Phys. 119 (8) (Feb. 2016) 083105, https://doi.org/10.1063/1.4942623.

[113] M. Borzenkov, P. Pallavicini, G. Chirico, Photothermally active inorganic nanoparticles: from colloidal solutions to photothermally active printed surfaces and polymeric nanocomposite materials, Eur. J. Inorg. Chem. 2019 (41) (2019) 4397–4404, https://doi.org/10.1002/ejic.201900836.

[114] J. Wang, et al., Synthesis of gold nanoflowers stabilized with amphiphilic daptomycin for enhanced photothermal antitumor and antibacterial effects, Int. J. Pharm. 580 (March) (2020), 119231, https://doi.org/10.1016/j.ijpharm.2020.119231.

[115] D.G. Meeker, et al., Synergistic photothermal and antibiotic killing of biofilm-associated Staphylococcus aureus using targeted antibiotic-loaded gold nanoconstructs, ACS Infect. Dis. 2 (4) (2016) 241–250, https://doi.org/10.1021/acsinfecdis.5b00117.

[116] S. Yu, et al., NIR-laser-controlled hydrogen-releasing PdH nanohydride for synergistic hydrogen-photothermal antibacterial and wound-healing therapies, Adv. Funct. Mater. 29 (50) (2019) 1–14, https://doi.org/10.1002/adfm.201905697.

[117] V. Agarwal, K. Chatterjee, Recent advances in the field of transition metal dichalcogenides for biomedical applications, Nanoscale 10 (35) (2018) 16365–16397, https://doi.org/10.1039/c8nr04284e.

[118] Y. Zhu, et al., Multicomponent transition metal dichalcogenide nanosheets for imaging-guided photothermal and chemodynamic therapy, Adv. Sci. 7 (23) (2020) 1–11, https://doi.org/10.1002/advs.202000272.

[119] C. Wang, J. Bai, Y. Liu, X. Jia, X. Jiang, Polydopamine coated selenide molybdenum: a new photothermal nanocarrier for highly effective chemo-photothermal synergistic therapy, ACS Biomater. Sci. Eng. 2 (11) (Nov. 2016) 2011–2017, https://doi.org/10.1021/acsbiomaterials.6b00416.

[120] A. Zhang, A. Li, W. Zhao, J. Liu, Recent advances in functional polymer decorated two-dimensional transition-metal dichalcogenides nanomaterials for chemo-photothermal therapy, Chem. - A Eur. J. 24 (17) (2018) 4215–4227, https://doi.org/10.1002/chem.201704197.

[121] E.A. Hussein, M.M. Zagho, G.K. Nasrallah, A.A. Elzatahry, Recent advances in functional nanostructures as cancer photothermal therapy, Int. J. Nanomedicine 13 (2018) 2897–2906, https://doi.org/10.2147/IJN.S161031.

[122] X. Song, Q. Chen, Z. Liu, Recent advances in the development of organic photothermal nano-agents, Nano Res. 8 (2) (2015) 340–354, https://doi.org/10.1007/s12274-014-0620-y.

[123] L. Cheng, K. Yang, Q. Chen, Z. Liu, Organic stealth nanoparticles for highly effective in vivo near-infrared Photothermal therapy of Cancer, ACS Nano 6 (6) (Jun. 2012) 5605–5613, https://doi.org/10.1021/nn301539m.

[124] M. Chu, et al., Near-infrared laser light mediated cancer therapy by photothermal effect of Fe3O4 magnetic nanoparticles, Biomaterials 34 (16) (May 2013) 4078–4088, https://doi.org/10.1016/j.biomaterials.2013.01.086.

[125] Z. Zhou, et al., Tungsten oxide nanorods: an efficient nanoplatform for tumor CT imaging and photothermal therapy, Sci. Rep. 4 (1) (May 2015) 3653, https://doi.org/10.1038/srep03653.

[126] G. Gao, Y.W. Jiang, H.R. Jia, F.G. Wu, Near-infrared light-controllable on-demand antibiotics release using thermo-sensitive hydrogel-based drug reservoir for combating bacterial infection, Biomaterials 188 (2019) 83–95, https://doi.org/10.1016/j.biomaterials.2018.09.045.

[127] J.-W. Xu, K. Yao, Z.-K. Xu, Nanomaterials with a photothermal effect for antibacterial activities: an overview, Nanoscale 11 (18) (2019) 8680–8691, https://doi.org/10.1039/C9NR01833F.

[128] B. Zhao, et al., A multifunctional platform with single-NIR-laser-triggered photothermal and NO release for synergistic therapy against multidrug-resistant gram-negative bacteria and their biofilms, J. Nanobiotechnol. 18 (1) (2020) 1–25, https://doi.org/10.1186/s12951-020-00614-5.

[129] K. Wang, et al., Self-assembled IR780-loaded transferrin nanoparticles as an imaging, targeting and PDT/PTT agent for cancer therapy, Sci. Rep. 6 (1) (Jul. 2016) 27421, https://doi.org/10.1038/srep27421.

[130] Y. Zhang, et al., Near-infrared light-activated thermosensitive liposomes as efficient agents for photothermal and antibiotic synergistic therapy of bacterial biofilm, ACS Appl. Mater. Interfaces 10 (17) (2018) 14426–14437, https://doi.org/10.1021/acsami.8b01327.

[131] X. Wang, et al., Multi-responsive photothermal-chemotherapy with drug-loaded melanin-like nanoparticles for synergetic tumor ablation, Biomaterials 81 (Mar. 2016) 114–124, https://doi.org/10.1016/j.biomaterials.2015.11.037.

[132] M. Xu, et al., Near-infrared-controlled nanoplatform exploiting photothermal promotion of peroxidase-like and OXD-like activities for potent antibacterial and anti-biofilm therapies, ACS Appl. Mater. Interfaces 12 (45) (2020) 50260–50274, https://doi.org/10.1021/acsami.0c14451.

[133] M.Q. Mesquita, C.J. Dias, M.G.P.M.S. Neves, A. Almeida, M.A.F. Faustino, Revisiting current photoactive materials for antimicrobial photodynamic therapy, Molecules 23 (10) (2018), https://doi.org/10.3390/molecules23102424.

[134] A. Fraix, S. Sortino, Combination of PDT photosensitizers with NO photodononors, Photochem. Photobiol. Sci. 17 (11) (2018) 1709–1727, https://doi.org/10.1039/c8pp00272j.

[135] N.E. Eleraky, A. Allam, S.B. Hassan, M.M. Omar, Nanomedicine fight against antibacterial resistance: An overview of the recent pharmaceutical innovations, Pharmaceutics 12 (2) (2020) 1–51, https://doi.org/10.3390/pharmaceutics12020142.

[136] A. Wozniak, M. Grinholc, Combined antimicrobial activity of photodynamic inactivation and antimicrobials-state of the art, Front. Microbiol. 9 (May) (2018), https://doi.org/10.3389/fmicb.2018.00930.

[137] A.W. Girotti, Photosensitized oxidation of membrane lipids: reaction pathways, cytotoxic effects, and cytoprotective mechanisms, J. Photochem. Photobiol. B Biol. 63 (1–3) (Oct. 2001) 103–113, https://doi.org/10.1016/S1011-1344(01)00207-X.

[138] A. Almeida, M.A. Faustino, J.P. Tomé, Photodynamic inactivation of bacteria: finding the effective targets, Future Med. Chem. 7 (10) (Jul. 2015) 1221–1224, https://doi.org/10.4155/fmc.15.59.

[139] V. Pérez-Laguna, A.J. García-Malinis, C. Aspiroz, A. Rezusta, Y. Gilaberte, Antimicrobial effects of photodynamic therapy, G. Ital. di Dermatologia e Venereol. 153 (6) (Dec. 2018), https://doi.org/10.23736/S0392-0488.18.06007-8.

[140] J. Ghorbani, D. Rahban, S. Aghamiri, A. Teymouri, A. Bahador, Photosensitizers in antibacterial photodynamic therapy: an overview, Laser Ther. 27 (4) (2018) 293–302, https://doi.org/10.5978/islsm.27_18-RA-01.

[141] M.T. Pelegrino, R.B. Weller, X. Chen, J.S. Bernardes, A.B. Seabra, Chitosan nanoparticles for nitric oxide delivery in human skin, Medchemcomm 8 (4) (2017) 713–719, https://doi.org/10.1039/C6MD00502K.

[142] C.-H. Su, et al., Enhancing microcirculation on multitriggering manner facilitates angiogenesis and collagen deposition on wound healing by photoreleased NO from hemin-Derivatized colloids, ACS Nano 13 (4) (Apr. 2019) 4290–4301, https://doi.org/10.1021/acsnano.8b09417.

[143] B.J. Privett, A.D. Broadnax, S.J. Bauman, D.A. Riccio, M.H. Schoenfisch, Examination of bacterial resistance to exogenous nitric oxide, Nitric Oxide 26 (3) (Mar. 2012) 169–173, https://doi.org/10.1016/j.niox.2012.02.002.

[144] D. Hu, Y. Deng, F. Jia, Q. Jin, J. Ji, Surface charge switchable supramolecular nanocarriers for nitric oxide synergistic photodynamic eradication of biofilms, ACS Nano 14 (1) (Jan. 2020) 347–359, https://doi.org/10.1021/acsnano.9b05493.

[145] S. Fayad-Kobeissi, et al., Vascular and angiogenic activities of CORM-401, an oxidant-sensitive CO-releasing molecule, Biochem. Pharmacol. 102 (Feb. 2016) 64–77, https://doi.org/10.1016/j.bcp.2015.12.014.

[146] Z. Wang, et al., Light controllable chitosan micelles with ROS generation and essential oil release for the treatment of bacterial biofilm, Carbohydr. Polym. 205 (2019) 533–539, https://doi.org/10.1016/j.carbpol.2018.10.095.

[147] D.J. Overstreet, et al., Temperature-responsive PNDJ hydrogels provide high and sustained antimicrobial concentrations in surgical sites, Drug Deliv. Transl. Res. 9 (4) (Aug. 2019) 802–815, https://doi.org/10.1007/s13346-019-00630-5.

[148] T. Liu, et al., Evaluation of the anti-biofilm effect of poloxamer-based thermoreversible gel of silver nanoparticles as a potential medication for root canal therapy, Sci. Rep. 11 (1) (Dec. 2021) 12577, https://doi.org/10.1038/s41598-021-92081-7.

[149] H. Choi, A. Schulte, M. Müller, M. Park, S. Jo, H. Schönherr, Drug release from Thermo-responsive polymer brush coatings to control bacterial colonization and biofilm growth on titanium implants, Adv. Healthc. Mater. 10 (11) (Jun. 2021) 2100069, https://doi.org/10.1002/adhm.202100069.

[150] A. Baki, F. Wiekhorst, R. Bleul, Advances in magnetic nanoparticles engineering for biomedical applications—a review, Bioengineering 8 (10) (2021), https://doi.org/10.3390/bioengineering8100134.

[151] E.C. Abenojar, et al., Magnetic glycol chitin-based hydrogel nanocomposite for combined thermal and d -amino-acid-assisted biofilm disruption, ACS Infect. Dis. 4 (8) (2018) 1246–1256, https://doi.org/10.1021/acsinfecdis.8b00076.

[152] X. Hua, S. Tan, H.M.H.N. Bandara, Y. Fu, S. Liu, H.D.C. Smyth, Externally controlled triggered-release of drug from PLGA micro and nanoparticles, PLoS One 9 (12) (2014) 1–17, https://doi.org/10.1371/journal.pone.0114271.

[153] R. Nickel, M.R. Kazemian, Y. Wroczynskyj, S. Liu, J. Van Lierop, Exploiting shape-selected iron oxide nanoparticles for the destruction of robust bacterial biofilms-active transport of biocides: via surface charge and magnetic field control, Nanoscale 12 (7) (2020) 4328–4333, https://doi.org/10.1039/c9nr09484a.

[154] Y. Ji, et al., Enhanced eradication of bacterial/Fungi biofilms by glucose oxidase-modified magnetic nanoparticles as a potential treatment for persistent endodontic infections, ACS Appl. Mater. Interfaces 13 (15) (2021) 17289–17299, https://doi.org/10.1021/acsami.1c01748.

[155] S. Obuobi, A. Ngoc Phung, K. Julin, M. Johannessen, N. Škalko-Basnet, Biofilm responsive Zwitterionic antimicrobial nanoparticles to treat cutaneous infection, Biomacromolecules (2021), https://doi.org/10.1021/acs.biomac.1c01274.

[156] Z. Wang, et al., Pd-cu nanoalloy for dual stimuli-responsive chemo-photothermal therapy against pathogenic biofilm bacteria, Acta Biomater. 137 (2022) 276–289, https://doi.org/10.1016/j.actbio.2021.10.028.

[157] M.M. Lu, et al., Redox/pH dual-controlled release of chlorhexidine and silver ions from biodegradable mesoporous silica nanoparticles against oral biofilms, Int. J. Nanomedicine 13 (2018) 7697–7709, https://doi.org/10.2147/IJN.S181168.

[158] A. Lianou, G.J.E. Nychas, K.P. Koutsoumanis, Strain variability in biofilm formation: a food safety and quality perspective, Food Res. Int. 137 (June) (2020), 109424, https://doi.org/10.1016/j.foodres.2020.109424.

[159] D. Peng, et al., Fabrication of pH responsive core-shell nanosystem with low-temperature photothermal therapy effect for treating bacterial biofilm infection, Biomater. Sci. (2021), https://doi.org/10.1039/d1bm01329g.

[160] H. Ji, et al., Bacterial hyaluronidase self-triggered prodrug release for chemo-photothermal synergistic treatment of bacterial infection, Small 12 (45) (Dec. 2016) 6200–6206, https://doi.org/10.1002/smll.201601729.

[161] D. Yang, et al., A lipase-responsive antifungal nanoplatform for synergistic photodynamic/photothermal/pharmaco-therapy of azole-resistant Candida albicans infections, Chem. Commun. 55 (100) (2019) 15145–15148, https://doi.org/10.1039/C9CC08463K.

[162] H. Han, et al., Biofilm microenvironment activated supramolecular nanoparticles for enhanced photodynamic therapy of bacterial keratitis, J. Control. Release 327 (Nov. 2020) 676–687, https://doi.org/10.1016/j.jconrel.2020.09.014.

[163] X. Wang, et al., Microenvironment-responsive magnetic nanocomposites based on Silver nanoparticles/gentamicin for enhanced biofilm disruption by magnetic field, ACS Appl. Mater. Interfaces 10 (41) (2018) 34905–34915, https://doi.org/10.1021/acsami.8b10972.

[164] Y. Liu, Y. Li, L. Shi, Controlled drug delivery systems in eradicating bacterial biofilm-associated infections, J. Control. Release 329 (2021) 1102–1116, https://doi.org/10.1016/j.jconrel.2020.10.038.

[165] Y. Liu, et al., Nanocarriers with conjugated antimicrobials to eradicate pathogenic biofilms evaluated in murine in vivo and human ex vivo infection models, Acta Biomater. 79 (2018) 331–343, https://doi.org/10.1016/j.actbio.2018.08.038.

[166] M. Ghosh, et al., In vitro and in vivo genotoxicity of silver nanoparticles, Mutat. Res. Genet. Toxicol. Environ. Mutagen. 749 (1–2) (2012) 60–69, https://doi.org/10.1016/j.mrgentox.2012.08.007.

[167] Z. Wang, Z. Wang, Nanoparticles induced embryo–fetal toxicity, Toxicol. Ind. Health 36 (3) (Mar. 2020) 181–213, https://doi.org/10.1177/0748233720918689.

[168] W. Najahi-Missaoui, R.D. Arnold, B.S. Cummings, Safe nanoparticles: are we there yet? Int. J. Mol. Sci. 22 (1) (2021) 1–22, https://doi.org/10.3390/ijms22010385.

[169] M. Horie, Y. Tabei, Role of oxidative stress in nanoparticles toxicity, Free Radic. Res. 55 (4) (Apr. 2021) 331–342, https://doi.org/10.1080/10715762.2020.1859108.

[170] De Jong, Drug delivery and nanoparticles: applications and hazards, Int. J. Nanomedicine (Jun. 2008) 133, https://doi.org/10.2147/IJN.S596.

[171] Y.N. Zhang, W. Poon, A.J. Tavares, I.D. McGilvray, W.C.W. Chan, Nanoparticle–liver interactions: cellular uptake and hepatobiliary elimination, J. Control. Release 240 (2016) 332–348, https://doi.org/10.1016/j.jconrel.2016.01.020.

[172] J. Wolfram, et al., Safety of nanoparticles in medicine, Curr. Drug Targets 16 (14) (Nov. 2015) 1671–1681, https://doi.org/10.2174/1389450115666140804124808.

[173] S.M. Moghimi, I.S. Muir, L. Illum, S.S. Davis, V. Kolb-Bachofen, Coating particles with a block co-polymer (poloxamine-908) suppresses opsonization but permits the activity of dysopsonins in the serum, BBA - Mol. Cell Res. 1179 (2) (1993) 157–165, https://doi.org/10.1016/0167-4889(93)90137-E.

[174] D. Boraschi, et al., Nanoparticles and innate immunity: new perspectives on host defence, Semin. Immunol. 34 (August) (2017) 33–51, https://doi.org/10.1016/j.smim.2017.08.013.

[175] L. Ding, Z. Liu, M. Aggrey, C. Li, J. Chen, L. Tong, Nanotoxicity: the toxicity research progress of metal and metal- containing nanoparticles, Mini-Rev. Med. Chem. 15 (7) (2015) 529–542, https://doi.org/10.2174/1389557515107150424104334.

[176] Ž. Vanić, M.W. Jøraholmen, N. Škalko-Basnet, Nanomedicines for the topical treatment of vulvovaginal infections: addressing the challenges of antimicrobial resistance, Adv. Drug Deliv. Rev. 178 (Nov. 2021), 113855, https://doi.org/10.1016/j.addr.2021.113855.

[177] C. Yang, et al., Nanoparticles in ocular applications and their potential toxicity, Front. Mol. Biosci. 9 (July) (2022) 1–18, https://doi.org/10.3389/fmolb.2022.931759.

[178] J. du Plessis, C. Ramachandran, N. Weiner, D. Muller, The influence of particle size of liposomes on the deposition of drug into skin, Int. J. Pharm. 103 (3) (Mar. 1994) 277–282, https://doi.org/10.1016/0378-5173(94)90178-3.

[179] L. Zhao, X. Zhang, X. Wang, X. Guan, W. Zhang, J. Ma, Recent advances in selective photothermal therapy of tumor, J. Nanobiotechnol. 19 (1) (2021) 1–15, https://doi.org/10.1186/s12951-021-01080-3.